tion for novel antitumor therapy. *In vivo* animal studies have shown that systemic administration of α-GalCer can lead to anti-tumor effects against various tumors (including melanoma, sarcoma, colon carcinoma, and lymphoma) in hepatic and lung metastasis models.[20,21] Intravenous administration of α-GalCer pulsed DCs leads to more potent anti-tumor activities than direct administration of α-GalCer alone in mouse metastatic tumor models.[18,22] Based on the promising results of preclinical studies demonstrating the antitumor potential of α-GalCer, several phase I clinical studies have been done in cancer immunotherapy using intravenous administration of α-GalCer or α-GalCer-loaded DCs, but with limited clinical responses.[23-26] This might partly be because intravenous administered α-GalCer or α-GalCer-loaded DCs may not be delivered efficiently to the tumor site. Although the antitumor effect of α-GalCer has been demonstrated in murine metastatic liver tumor,[20-22,27] no clinical trial against liver cancer has been reported to date. For further development of liver cancer treatment, intrahepatic (i.h.) injection of α-GalCer-loaded DCs, expected to be the most efficient delivery system for tumor lesions, should be tested with respect to inducing effective antitumor therapy.

In this study, we evaluated the antitumor effect of i.h. injection of α-GalCer-pulsed DCs in murine liver tumor. Compared to the conventional peptide-pulsed DC vaccine, we observed effective antitumor effects against not only liver tumor but also disseminated tumor via more efficient activation of innate and acquired immunity in the liver.

Materials and Methods

Mice. Six- to eight-week-old female BALB/c mice were purchased from Shizuoka Experimental Animal Laboratory (Shizuoka, Japan), and maintained in microisolator cages. The animals were handled under aseptic conditions. Procedures were performed according to approved protocol and in accordance with recommendations for the proper care and use of laboratory animals.

Cell Lines and $p53_{232-240}$ Peptide. CMS4 sarcomas ($H\text{-}2^d$) express mutated p53 and present the wild-type $p53_{232-240}$ epitope recognized by $H\text{-}2K^d$-resticted CTL.[28] Colon26, a mouse colon adenocarcinoma cell line, was kindly provided by Dr. Takashi Tsuruo (Institute of Molecular and Cellular Bioscience, University of Tokyo, Tokyo, Japan). These cell lines were maintained in complete media (CM), which is RPMI-1640 medium supplemented with 10% heat-inactivated fetal bovine serum, 100 U/ml penicillin, 100 μg/ml streptomycin, and 10 mM L-glutamine (all reagents from GIBCO/Life Technologies, Grand Island, NY), in a humidified incubator at 5% CO_2 and 37°C.

α-GalCer. Alpha-GalCer was kindly provided by Kirin Brewery (Gunma, Japan) and prepared as described by Kawano et al.[9]

Preparation of α-GalCer-Pulsed DCs or p53 Peptide-Pulsed DCs. Bone marrow derived DCs were generated from BALB/c mice as previously described with minor modification.[29] Briefly, BALB/c bone marrow was cultured in CM supplemented with 1000 U/ml of rmGM-CSF and 1000 U/ml of rmIL-4 (PeproTech EC, London, UK) for 7 days. CD11c+ dendritic cells were isolated from whole bone marrow culture by magnetic cell sorting using MACS (Miltenyi Biotec, Gladbach, Germany) according to the manufacturer's protocol. DCs typically represented >90% of the harvested population of cells based on the morphology and expression of the CD11b, CD11c, CD40, CD80, CD86, and class II MHC antigens (data not shown). On day 7, DCs were added to α-GalCer (100 ng/ml) and cultured for 24 hours to prepare α-GalCer-pulsed DCs (αGCDC). To prepare p53 peptide-pulsed DCs (pepDC), the mouse $p53_{232-240}$ peptide was added to day 7 DCs as described.[28] Alpha-GCDC or pepDC were then washed twice with PBS before i.h. injection of these cells.

Animal Experiments. BALB/c mice were intrahepatically injected with 5×10^5 CMS4 cells and 1×10^6 αGCDC, pepDC, or DCs in a total volume of 100 μl of phosphate-buffered saline (PBS) on day 0. Two weeks after the tumor injection, the livers of the treated mice were removed, and the weight was measured to examine intrahepatic tumor growth. To assess the impact of systemic immunity from i.h. injection of αGCDC, BALB/c mice were injected intrahepatically with 5×10^5 CMS4 cells or Colon26 cells and 1×10^6 αGCDC. On day 28 after i.h. injection, 1×10^6 CMS4 cells or Colon26 cells were injected into the right flank of treated mice. Tumor size was assessed every 3 or 4 days and recorded in square millimeters by determining the product of the largest perpendicular diameters measured using vernier calipers. Data are reported as the average tumor area ± SD.

IFN-γ ELISA. Mice sera were harvested 2 weeks after intrahepatic tumor injection and αGCDC or pepDC treatment, and subjected to mouse IFN-γ ELISA (BD-Pharmingen, San Diego, CA), with lower levels of detection of 31.3 pg/ml.

Cytotoxic Assay. BALB/c mice were treated with an i.h. injection of 1×10^6 αGCDC, pepDC or DCs. After 48 hours, hepatic mononuclear cells (MNCs) were prepared as previously described.[20] To evaluate the cytotoxicity of hepatic NK cells, WST-8 [2-(2-methoxy-4-nitrophenyl)-3-(4-nitrophenyl)-5-(2,4-disulfophenyl)-

2H-tetrazolium, monosodium, salt] assay (Nacalai Tesque, Kyoto, Japan) was performed as described with minor modification.[29] After 24 hours of coculture of hepatic MNC and NK-susceptible YAC-1 target cells at the 5:1 ratio (hepatic MNC:YAC-1 cells) in 96-well plates, 10 μl WST-8 was added to each well and the cells were incubated for another 1 hour. The 450 nm absorbance was measured using a microplate reader (Benchmark, Bio-Rad Laboratories, CA). NK cell cytotoxicity was calculated as described.[29]

CD8+ T Cell Response Against $p53_{232\text{-}240}$ Peptide. On day 14 after i.h. injection of CMS4 cells and αGCDC or pepDC, CD8+ T cells were isolated from the spleen cells of treated mice bearing CMS4 liver tumor by using magnetic beads (MACS) and then were cocultured (1×10^5 cells/well) with syngeneic DCs (2×10^4 cells/well) pulsed with or without $p53_{232\text{-}240}$ peptide in 96-well tissue culture plate. After 48 hours incubation, the culture supernatant was collected and analyzed for IFN-γ release using specific ELISA kit (BD-Pharmingen).

T Cell and NK Cell Depletion Experiments. On days −6, −1, 5, and 10 after tumor inoculation, mice were injected intraperitoneally with anti-CD4 [GK1.5 hybridoma, American Type Culture Collection (ATCC), Manassas, VA] or anti-CD8 (53-6.72 hybridoma, ATCC) as described.[29] The efficiency of specific subset depletions was validated by flow cytometry analysis of splenocytes using PE-conjugated anti-CD4 and anti-CD8 mAbs (Pharmingen). For NK cell depletion, mice were injected with anti-asialo GM-1 (Wako, Osaka, Japan) on day −1, 5, and 10 after tumor inoculation. The efficiency of NK cell depletion was validated by flow cytometry analysis of splenocytes using PE-conjugated anti-DX5 mAbs (Pharmingen). In all cases, 99% of the targeted cell subset was specifically depleted (data not shown).

Statistical Analysis. The statistical significance of differences between the groups was determined by applying the Student t test or 2-sample *t* test with Welch correction after each group had been tested with equal variance and Fisher's exact probability test. The statistical significance of the differences in more than 2 groups was determined by applying one-way ANOVA. Survival reliability was estimated from the Kaplan-Meier curve, and statistics were analyzed by the log rank test. We defined statistical significance as $P < 0.05$.

Results

Intrahepatic Delivery of αGCDC Is More Therapeutic Than pepDC in the CMS4 Liver Tumor Model. We examined the therapeutic potential of αGCDC or pepDC against CMS4 liver tumor. DCs were generated from bone marrow cells and pulsed with α-GalCer or $p53_{232\text{-}240}$ peptide. BALB/c mice were injected intrahepatically with 5×10^5 CMS4 cells and 1×10^6 αGCDC, pepDC, DCs only or PBS. Two weeks after the tumor injection, the livers of the treated mice were removed, and the weight was measured to examine intrahepatic tumor growth. Large CMS4 tumors formed in all mice treated with either PBS or DCs (Fig. 1A). Small CMS4 tumors formed in the liver of pepDC treated mice, with the exception of 1 mouse among the 6 pepDC-treated mice. No tumor formation was observed in the liver of any of the αGCDC-treated mice. The liver weight of the pepDC treatment group tended to be lighter than that of the PBS treatment group, but not with statistical significance. The liver weight of the αGCDC treatment group was significantly lighter than that of the PBS treatment groups (Fig. 1B). The survival rate of the pepDC-treated group was significantly higher than those of the DC-treated or PBS-treated groups ($P < 0.05$) whereas that of the DC-treated group was not significantly different from that of the PBS-treated group. All αGCDC-treated mice survived at 70 days after tumor inoculation, but all pepDC-treated mice died within 35 days (Fig. 1C). These results suggested that the αGCDC treatment has more therapeutic potential against CMS4 liver tumor than conventional pepDC treatment. Therapeutic potential of αGCDC is not unique to CMS4 liver tumor model, because no Colon26 liver tumor was observed in mice treated with αGCDC and the liver weight of αGCDC-treated mice was significantly lighter than that of PBS-treated mice (Fig. 2).

Serum IFN-γ Level and Hepatic NK Cell Activation Are Associated with the Degree of Therapeutic Effect. We next evaluated whether the therapeutic benefits observed in our DC-based treatment regimens were associated with the degree of serum IFN-γ in treated animals. Mice serum was harvested 2 weeks after intrahepatic tumor injection and αGCDC or pepDC treatment, and subjected to mouse IFN-γ ELISA. Serum IFN-γ levels were elevated in αGCDC-treated and pepDC-treated mice, whereas no IFN-γ was detected in PBS-treated mice, mice treated with DCs only, or normal nontreated mice (Fig. 3A). The serum IFN-γ of αGCDC-treated mice was significantly higher than that of pepDC-treated mice,

To examine whether hepatic NK cells were actually activated by i.h. injection of αGCDC or pepDC, we examined the cytotoxic activity of hepatic MNC against YAC-1 cells after i.h. injection of αGCDC or pepDC. The cytotoxic activity of αGCDC-treated mice was significantly stronger than those of pepDC-treated, DC-treated, or PBS-treated mice (Fig. 3B).

These results indicated that i.h. injection of αGCDC in the liver could induce IFN-γ production in treated

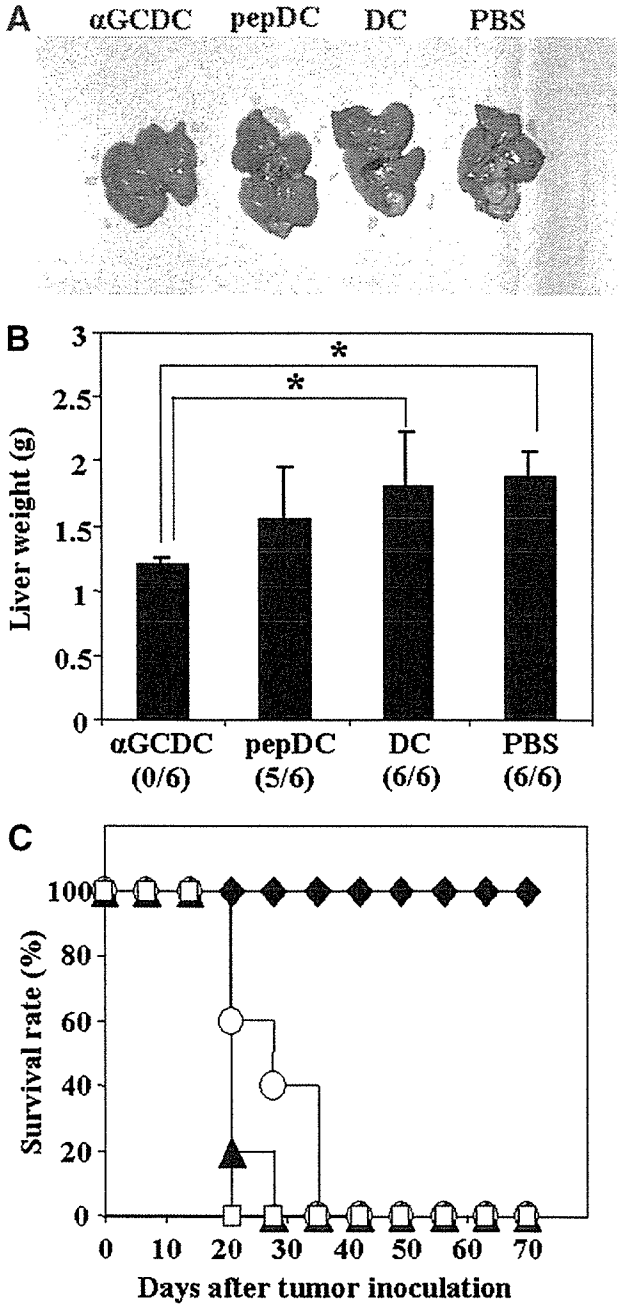

Fig. 1. Improved therapeutic effectiveness of i.h. delivered α-GalCer-pulsed DCs in CMS4 liver tumor model. BALB/c mice were injected intrahepatically with 5×10^5 CMS4 cells and 1×10^6 α-GalCer-pulsed DCs (αGCDC), $p53_{232\text{-}240}$ peptide-pulsed DCs (pepDC), DCs only (DC), or PBS (n = 6 in each treatment group). Two weeks after the CMS4 tumor injection, the livers were removed from all treated mice. (A) Representative liver macroscopic view of each group. (B) Comparison of liver weight of each group. As a control, the mean liver weights of untreated normal mice were 1.11 ± 0.05 g. $^*P < 0.05$. In all cases, the fraction of mice bearing liver tumor in each treatment group at 14 days is given in parentheses. (C) Survival curve of mice intrahepatically inoculated with CMS4 cells. CMS4 liver tumor bearing mice were treated with αGCDC (solid diamonds), pepDC (empty circles), DC (solid triangles), or PBS (empty squares) (n = 10 in each treatment group).

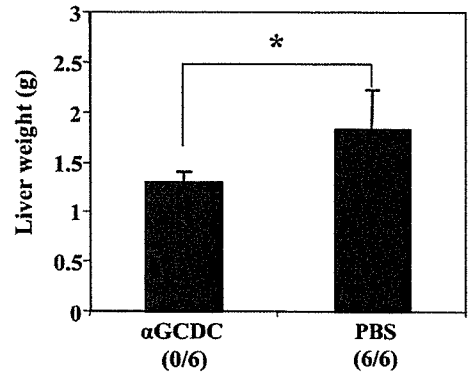

Fig. 2. Improved therapeutic effectiveness of i.h. delivered α-GalCer-pulsed DCs in Colon26 liver tumor model. BALB/c mice were injected intrahepatically with 5×10^5 Colon26 cells and 1×10^6 α-GalCer-pulsed DCs (αGCDC) or PBS (n = 6 in each treatment group). Two weeks after the Colon26 tumor injection, the livers were removed from all treated mice. As a control, the mean liver weights of untreated normal mice were 1.11 ± 0.05 g. Comparison of liver weight of each group. $^*P < 0.05$. In all cases, the fraction of mice bearing liver tumor in each treatment group at 14 days is given in parentheses.

mice and efficiently activate hepatic NK cells, suggesting that there may be an association between IFN-γ production or NK cell activation and the degree of therapeutic effects observed in this system.

Depletion of NK Cells Abolishes the Antitumor Effect of αGCDC. To verify that the therapeutic benefit of αGCDC-based regimen in the CMS4 liver tumor model was T cell-dependent and NK cell-dependent, we performed T cell subset depletion and NK cell depletion studies (Fig. 4). NK cell depletions significantly inhibited the therapeutic efficacy of i.h. injections with αGCDC ($P < 0.05$ versus NK cell-depleted mice). In contrast, neither CD4+ nor CD8+ T cell depletions inhibited the therapeutic efficacy of i.h. injection with αGCDC. These results suggested that NK cells, but neither CD8+ nor CD4+ T cells, play critical roles in the antitumor effect against mouse liver tumor.

$p53_{232\text{-}240}$ Peptide-Specific CTLs Are Generated After DC Treatment of Liver Tumor. We next evaluated whether $p53_{232\text{-}240}$ peptide-specific CTLs were generated after treatment of liver tumor by DC treatment. CD8+ T cells were isolated from the spleen cells of treated mice and then cocultured with syngeneic DCs pulsed with $p53_{232\text{-}240}$ peptide strongly expressed on CMS4 cells. The $p53_{232\text{-}240}$ peptide-specific IFN-γ production of CD8+ T cells differed significantly among the treatment groups (Fig. 5). CD8+ T cells from mice treated with αGCDC produced higher levels of the Th-1 associated cytokine IFN-γ in response to $p53_{232\text{-}240}$ peptide than CD8+ T cells obtained from mice treated with any other DC-based vaccine or with

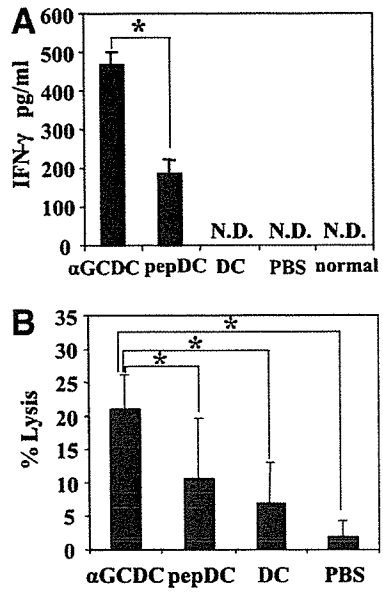

Fig. 3. Increase in serum IFN-γ levels and activation of hepatic NK cells in mice treated with αGCDC. (A) Mice sera were harvested two weeks after intrahepatic CMS4 tumor injection and treatments of αGCDC, pepDC treatment, DC only, or PBS, and subjected to IFN-γ ELISA. Naïve mice (normal) were used as controls. Cytokine levels are reported in picograms per milliliter (mean ± SD of triplicate samples). Similar results were obtained in 2 independent experiments. N.D., not detected. $*P < 0.05$. (B) BALB/c mice were treated with an i.h. injection of 1×10^6 αGCDC, pepDC, DC only, or PBS. After 48 hours, hepatic mononuclear cells were isolated from the liver to evaluate the cytotoxicity against YAC-1 cells at 5:1 effector/target cells ratio. Similar results were obtained in 2 independent experiments. $*P < 0.05$.

PBS only, suggesting that strong $p53_{232\text{-}240}$ peptide-specific CTLs were generated by αGCDC treatment of the liver tumor.

Systemic Therapeutic Antitumor Immunity Is Induced by i.h. Injection with αGCDC. Because strong anti-CMS4 CTL response was generated in αGCDC-treated animals, we next chose to analyze whether treatment of a CMS4 lesion in the liver would affect the growth of rechallenged CMS4 tumors. BALB/c mice were intrahepatically injected with CMS4 tumors and αGCDC. After 28 days, 1×10^6 CMS4 cells or Colon26 cells were injected subcutaneously in the right flank. The subcutaneous CMS4 tumors in mice receiving the αGCDC regimen were completely rejected in all mice (Fig. 6A). The growth of subcutaneous Colon26 tumor in αGCDC-treated mice was not inhibited, suggesting that CMS4 specific antitumor immunity could be induced (Fig. 6B) by αGCDC treatment. Acquired immune responses induced by αGCDC is not unique to CMS4 tumor model, because the subcutaneous tumor growth of Colon26 cells (Fig. 6D), but not CMS4 cells (Fig. 6C), were also significantly inhibited in mice that had been

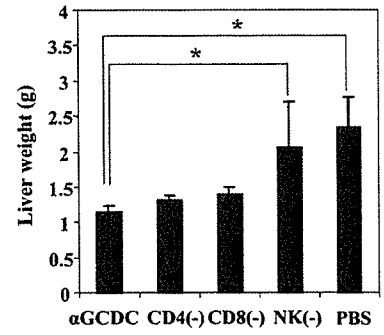

Fig. 4. Dependence of antitumor efficacy of i.h. αGCDC delivery on NK cells, not on CD4+ or CD8+ T cells. To prove that the therapeutic benefit of αGCDC-based regimen in the CMS4 liver tumor model is T cell-dependent and NK cell-dependent, the liver weights of αGCDC treated mice with $CD4^+$ (CD4(-)) and $CD8^-$ (CD8(-)) T cell subset or NK cell (ASGM1) depletion or without depletion (αGCDC) were shown. The liver weights of mice treated with PBS were also shown. As a control, the mean liver weights of untreated normal mice were 1.11 ± 0.05 g. Ab-mediated *in situ* depletion of NK cells, but not $CD4^+$ or $CD8^+$ T cells, markedly reduced the therapeutic efficacy of αGCDC therapy (n = 6 in each treatment group). $*P < 0.05$ versus αGCDC.

protected Colon26 liver tumor by i.h. injection of αGCDC.

Discussion

Tumor associated antigen derived peptide-pulsed DCs-based vaccine have been reported in various mouse tumor models,[30,31] and clinical applications of peptide-pulsed DCs have been tried with various cancer patients.[5,32-34] However, although tumor-specific T cells were promoted by vaccination in most patients, objective clinical responses have thus far only been observed in a

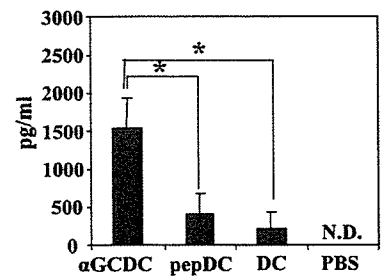

Fig. 5. Evaluation of $p53_{232\text{-}240}$ peptide specific CD8+ CTL in responder mice. CD8+ T cells were isolated from the spleen of mice 14 days after i.h. injection with DCs (αGCDC, α-GalCer pulsed DCs; pepDC, $p53_{232\text{-}240}$ peptide pulsed DCs; DC, DCs only; PBS, control) and CMS4 cells. IFN-γ production from CD8+ T cells against $p53_{232\text{-}240}$ peptide was measured by ELISA (results in picograms per milliliter; mean ± SD of triplicate samples). Syngeneic DCs pulsed with $p53_{232\text{-}240}$ peptide served as the antigen-presenting cells. IFN-γ production from CD8+ T cells against peptide-unpulsed syngeneic DCs served as negative control, and this value was subtracted from all experimental determinations to determine $p53_{232\text{-}240}$ peptide specific IFN-γ production. Similar results were obtained in two independent experiments. N.D., not detected. $*P < 0.05$.

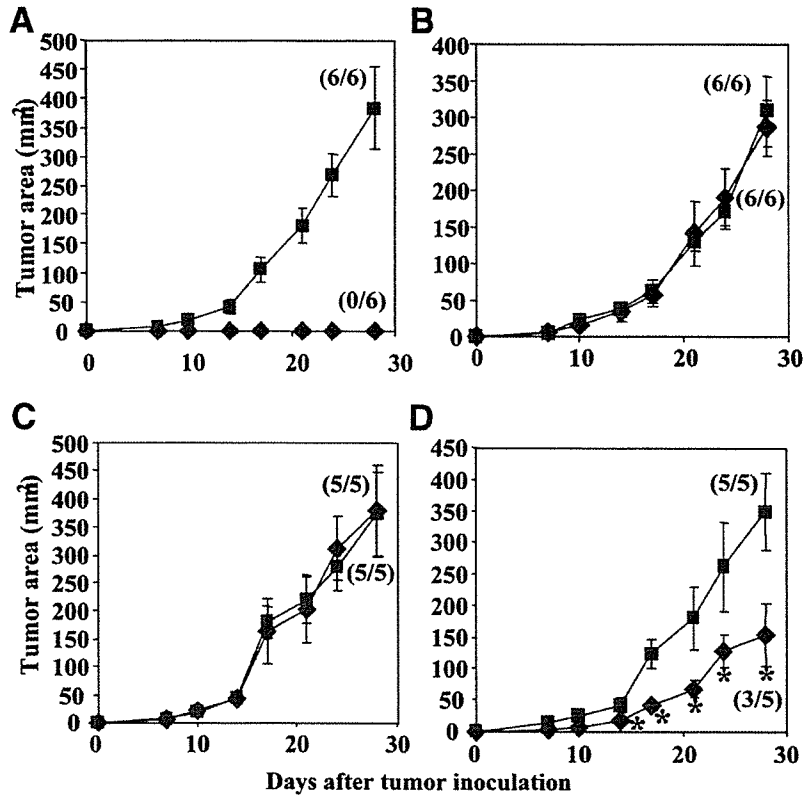

Fig. 6. Alpha-GCDC–based intrahepatic therapy results in the development of systemic anti-tumor immunity that protects distal tumor rechallenge. On day 0, BALB/c mice were injected intrahepatically with αGCDC and either CMS4 tumors (A, B, n = 6 in each treatment group)or Colon26 tumors (C, D, n = 5 in each treatment group). Twenty-eight days after treatment, mice were challenged subcutaneously with 1×10^6 CMS4 cells (A, C) or Colon26 cells (B, D) injected into the right flank. As a control, naïve mice were challenged with 1×10^6 CMS4 cells (A, C) or Colon26 cells (B, D).The fraction of mice bearing a tumor in each treatment group at day 28 is indicated in parentheses. Tumor size was expressed as the mean tumor size of only those mice bearing a tumor. αGCDC treated mice (solid diamonds); naive mice (solid squares). Each data point represents the mean tumor size ± SD. *$P < 0.05$. versus naive mice.

minority of treated individuals. A normal liver contains lymphocytes that are usually enriched with NK and NKT cells; i.e., 25% NK cells and 30% NKT cells in contrast to peripheral blood that contains only 10% NK and 5% NKT cells.[12,13] Recently, DCs have been implicated in the activation of NKT and NK cells in both mice and humans,[4-6,9-11,23,35] suggesting that activation of many innate immune cells in the liver by a DC-based vaccine would be promising for treating liver tumor. We hypothesize that i.h. injection of α-GalCer-pulsed DC can efficiently activate abundant innate immune cells in the liver and elicit effective innate and acquired immunity against liver tumor. Our results demonstrated that i.h. injection with αGCDC resulted in complete rejection of CMS4 liver tumors with prolonged survival of tumor-bearing mice whereas injection with pepDC did not. These results suggested the efficacy of i.h. injection of αGCDC for treating liver cancer and the superiority of αGCDC treatment over conventional pepDC treatment. Intrahepatic injection of αGCDC also revealed a strong antitumor effect in the Colon26 liver tumor model. Although DCs pulsed with both α-GalCer and peptide (αGC-pepDC) would be expected to provide a better therapy index, the therapeutic potential of αGC-pepDC was found to be similar with that of αGCDC in the CMS4 liver tumor model (Tatsumi T et al., unpublished data). These findings suggest that i.h. delivery of αGCDC may optimally promote antitumor effects in the mouse liver tumor microenvironment.

We have shown that serum IFN-γ was detected in αGCDC-treated and pepDC-treated mice and that serum IFN-γ levels in αGCDC-treated mice were significantly higher than in pepDC-treated mice. Zitvogel et al. reported that the antitumor effects of DC-based vaccination were dependent on the production of Th1-associated cytokines such as IFN-γ, tumor necrosis factor-α, and IL-12.[36] Therefore, enhanced IFN-γ production resulting from injection of αGCDC or pepDC into liver tumor may also play an important role in the antitumor activity in vivo. Our results also suggested that αGCDC treat-

ment in the liver could induce stronger antitumor immunity than pepDC treatment.

Efficient activation of abundant NKT cells and NK cells in the liver might be important in an antitumor effect against liver tumor. We and others have previously reported that sequential activation of NKT cells and NK cells could be observed in the liver after α-GalCer administration and that most NKT cells had disappeared from the liver within 12 hours of α-GalCer administration.[20,37] Thus, the activated NK cells mainly play critical roles in the antitumor effect of disseminated liver tumor.[20] We found that the NK cell activity of αGCDC-treated mice were significantly stronger than those of pepDC-treated, DC-treated, or PBS-treated mice. These findings offer evidence that intrahepatic injection of DCs activate hepatic NK cells and that αGCDC may activate liver abundant NK cells more efficiently than pepDC, which might be associated with the therapeutic outcomes of these treatments in liver tumors.

In this study, the depletion of NK cells, but not CD4+ or CD8+ T cells, diminished the antitumor effect against liver tumor by α-GalCer pulsed DCs. These results suggested that only NK cells play a critical role in eradication of mouse liver tumor by i.h. injection of αGCDC and that neither CD4+ nor CD8+ T cells play critical roles in the early phase of the eradication of liver tumor cells. However, our following results demonstrated that strong systemic acquired immunity could be generated after early eradication of liver tumor by treatment with αGCDC. These results suggested that NK cells activated by αGCDC might be the main effector cells in the early eradication of liver tumor cells and that liver tumor-derived tumor antigens are taken up by dedicated professional antigen-presenting cells in the liver, which might generate prolonged liver tumor antigen-specific acquired immunity.

Subsequent analyses revealed that CD8+ T cells isolated from mice treated with i.h. injection of αGCDC or pepDC in liver tumors secrete IFN-γ in response to $p53_{232\text{-}240}$ peptide strongly expressed on CMS4 cells when presented by syngeneic DCs *in vitro*. The IFN-γ level of CD8+ T cells from αGCDC-treated mice was much higher than that from pepDC-treated mice. Mayordomo et al. reported that immunization of $p53_{232\text{-}240}$ peptide-pulsed DCs induced peptide-specific CTL in immunized mice that showed cytolytic activity against CMS4, p53 overexpressing cells, and that $p53_{232\text{-}240}$ peptide-pulsed DC vaccine offered protection against CMS4 tumor challenge in mice.[28] These results suggested the therapeutic potential of $p53_{232\text{-}240}$ peptide-based DCs vaccine in the CMS4 tumor model. Our current data revealed that i.h. injection of αGCDC to liver tumors generated $p53_{232\text{-}240}$ peptide-specific CTL more efficiently than that of pepDC. The activation of NKT cells was associated with an expansion of antigen-specific CTL, as might be expected if the DCs that matured *in vivo* in response to NKT cells were capturing antigens.[38-41] In a clinical study, Chang et al. reported that increases of antigen-specific memory T cells were observed in cancer patients treated with α-GalCer-pulsed dendritic cells.[26] Our results suggested that the activation of hepatic NK cells in the liver might be associated with the efficiency of generation of tumor antigen-specific CTL. We believe that injection of αGCDC into the liver more efficiently activates innate immune cells, NKT cells and NK cells, followed by generation of tumor antigen-specific CTL than injection of pepDC.

Additional experiments using subcutaneous rechallenge with tumor demonstrated that i.h. αGCDC treatment of liver tumors not only blocked treated CMS4 liver tumor progression but offered complete protection against "recurrence" of the same tumor at a distant site. In contrast, Colon26 rechallenge tumor was not inhibited in the treated mice, suggesting that CMS4-specific immunity was generated after liver tumor treatment. These results were consistent with the activation of acquired immunity evaluated by IFN-γ secretion from CD8+ T cell in response to $p53_{232\text{-}240}$ peptide. Intrahepatic αGCDC treatment of Colon26 liver tumor also led to resistance to subsequent Colon26 challenge but not to CMS4 challenge. These data supported that i.h. αGCDC injection generally induced acquired immunity after rejection of original liver tumors. Taken together, we believe that i.h. αGCDC treatment of liver tumors offers the optimal therapeutic treatment for both local liver tumor and distant metastatic tumor.

In spite of recent progress and early successes reported for DC-based cancer immunotherapies, there remains significant room for improvement in these regimens, especially with respect to advanced liver cancer. The liver is the most common site of metastasis of gastrointestinal cancers (i.e. colorectal cancer, gastric cancer and pancreatic cancer). Thus, new therapeutic approaches of DC-based immunotherapy for advanced liver tumor need to be developed. Recently, percutaneous liver tumor ablation methods, radiofrequency ablation (RFA) therapy, and ethanol injection therapy (PEIT) have become well-established in hepatocellular carcinoma treatment. This encourages gastroenterologists to apply i.h. injection-immunotherapy to liver tumor treatment. We show here that i.h. injection of α-GalCer-pulsed DCs has greater antitumor efficacy than that of tumor antigen-derived peptide-pulsed DCs in liver cancer treatment and that i.h. injection of α-GalCer pulsed DCs into liver tumor results

in the coordinated activation of both innate and acquired immunity in the liver, leading to superior antitumor efficacy. These findings indicate that the use of i.h. delivery of α-GalCer-pulsed DCs might represent a particularly promising approach to suppressing tumor growth and promoting regression of metastatic lesions in liver cancer patients.

Acknowledgment: The authors thank the Pharmaceutical Research Laboratories, Kirin Brewery (Gunma, Japan) for providing the α-galactosylceramide.

References

1. Steinman RM. The dendritic cell system and its role in immunogenicity. Annu Rev Immunol 1991;9:271-296.
2. Hart DN. Dendritic cells: unique leukocyte populations which control the primary immune response. Blood 1997;90:3245-3287.
3. O'Neill DW, Adams S, Bhardwaj N. Manipulating dendritic cell biology for the active immunotherapy of cancer. Blood 2004;104:2235-2246.
4. Fernandez NC, Lozier A, Flament C, Ricciardi-Castagnoli P, Beller D, Suter M, et al. Dendritic cells directly trigger NK cell functions: cross-talk relevant in innate anti-tumor immune responses in vivo. Nat Med 1999; 5:405-411.
5. Gerosa F, Baldani-Guerra B, Nisii C, Marchesini V, Carra G, Trinchieri G. Reciprocal activating interaction between natural killer cells and dendritic cells. J Exp Med 2002;195:327-333.
6. Ferlazzo G, Tsang ML, Moretta L, Melioli G, Steinman RM, Munz C. Human dendritic cells activate resting NK cells and are recognized via the NKp30 receptor by activated NK cells. J Exp Med 2002;195:343-351.
7. Piccioli D, Sbrana S, Melandri E, Valiante NM. Contact-dependent stimulation and inhibition of dendritic cells by natural killer cells. J Exp Med 2002;195:335-341.
8. Miller G, Lahrs S, Dematteo RP. Overexpression of interleukin-12 enables dendritic cells to activate NK cells and confer systemic antitumor immunity. FASEB J 2003;17:728-730.
9. Kawano T, Cui J, Koezuka Y, Toura I, Kaneko Y, Motoki H, et al. CD1d-restricted and TCR-mediated activation of Vα14NKT cells by glycosylceramides. Science 1997;278:1626-1629.
10. Kawano T, Cui J, Koezuka Y, Toura I, Kaneko K, Sato H, et al. Natural killer-like nonspecific tumor cell lysis mediated by specific ligand-activated Vα14NKT cells. Proc Natl Acad Sci U S A 1998;95:5690-5693.
11. Kitamura H, Iwakabe K, Yahata T, Nishimura S, Ohta A, Ohmi S, et al. The natural killer T (NKT) cell ligand α-galactosylceramide demonstrates its immunopoteniating effect by inducing interleukin (IL)-12 production by dendritic cells and IL-12 receptor expression on NKT cells. J Exp Med 1999;189:1121-1128.
12. Doherty DG, O'Farrelly C. Innate and adaptive lymphoid cells in human liver. Immunol Rev 2000;174:5-20.
13. Mehal WZ, Azzaroli F, Crispe IN. Immunology of the healthy liver: Old questions and new insights. Gastroenterology 2001;120:250-260.
14. Ladhams A, Schmidt C, Sing G, Butterworth L, Fielding G, Tesar P, et al. Treatment of non-resectable hepatocellular carcinoma with autologous tumor-pulsed dendritic cells. J Gastroenterol Hepatol 2002;17:889-896.
15. Iwashita Y, Tahara K, Goto S, Sasaki A, Kai S, Seike M, et al. A phase I study of autologous dendritic cell-based immunotherapy for patients with unresectable primary liver cancer. Cancer Immunol Immunother 2003;52: 155-161.
16. Chi KH, Liu SJ, Li CP, Kuo HP, Wang YS, Chao Y, et al. Combination of conformal radiotherapy and intratumoral injection of adoptive dendritic cell immunotherapy in refractory hepatoma. J Immunother 2005;28:129-135.
17. Lee WC, Wang HC, Hung CF, Huang PF, Lia CR, Chen MF. Vaccination of advanced hepatocellular carcinoma patients with tumor lysate-pulsed dendritic cells: a clinical trial. J Immunother 2005;28:496-504.
18. Fujii S, Shimizu K, Kronenberg M, Steinman RM. Prolonged IFN-γ-producing NKT response induced with alpha-galactosylceramide-loaded DCs. Nat Immunol 2002;3:867-874.
19. Gonzalez-Aseguinolaza G, de Oliveira C, Tomaska M, Hong S, Bruna-Romero O, Nakayama T, et al. α-Galactosylceramide-activated Vα 14 natural killer T cells mediate protection against murine malaria. Proc Natl Acad Sci U S A 2000;97:8461-8466.
20. Miyagi T, Takehara T, Tatsumi T, Kanto T, Suzuki T, Jinushi M, et al. CD1d-mediated stimulation of natural killer T cells selectively activates hepatic natural killer cells to eliminate experimentally disseminated hepatoma cells in murine liver. Int J Cancer 2003;106:81-89.
21. Nakagawa R, Motoki K, Ueno H, Iijima R, Nakamura H, Kobayashi E, et al. Treatment of hepatic metastasis of the colon26 adenocacinoma with an α-galactosylceramide, KRN7000. Cancer Res 1998;58:1202-1207.
22. Toura I, Kawano T, Akutsu Y, Nakayama T, Ochiai T, Taniguchi M. Inhibition of experimental tumor metastasis by dendritic cells pulsed with α-galactosylceramide. J Immunol 1999;163:2387-2391.
23. Nieda M, Okai M, Tazbirkova A, Lin H, Yamaura A, Ide K, et al. Therapeutic activation of Vα24+Vβ11+NKT cells in human subjects results in highly coordinates secondary activation of acquired and innate immunity. Blood 2004;103:383-389.
24. Giaccone G, Punt CJ, Ando Y, Ruijter R, Nishi N, Peters M, et al. A phase I study of the natural killer T-cell ligand α-galactosylceramide (KRN7000) in patients with solid tumors. Clin Cancer Res 2002;8:3702-3709.
25. Ishikawa A, Motohashi S, Ishikawa E, Fuchida H, Higashino K, Otsuji M, et al. A phase I study of α-galactosylceramide (KRN7000)-pulsed dendritic cells in patients with advanced and recurrent non-small cell lung cancer. Clin Cancer Res 2005;11:1910-1917.
26. Chang DH, Osman K, Connolly J, Kukreja A, Krasovsky J, Pack M, et al. Sustained expansion of NKT cells and antigen-specific T cells after injection of α-galactosyl-ceramide loaded mature dendritic cells in cancer patients. J Exp Med 2005;201:1503-1517.
27. Chiodoni C, Stoppacciaro A, Sangaletti S, Gri G, Cappetti B, Koezuka Y, et al. Different requirements for α-galactosylceramide and recombinant interleukin-12 antitumor activity in the treatment of C-26 colon carcinoma hepatic metastases. Eur J Immunol 2001;31:3101-3110.
28. Mayordomo JI, Loftus DJ, Sakamoto H, De Cesare CM, Appasamy PM, Lotze MT, et al. Therapy of murine tumors with p53 wild-type and mutant sequence peptide-based vaccines. J Exp Med 1996;183:1357-1365.
29. Tatsumi T, Huang J, Gooding WE, Gambotto A, Robbins PD, Vujanovic NL, et al. Intratumoral delivery of dendritic cells engineered to secrete both interleukin(IL)-12 and IL-18 effectively treats local and distant disease in association with broadly reactive Tc1-type immunity. Cancer Res 2003; 63:6378-6386.
30. Porgador A, Snyder D, Gilboa E. Induction of antitumor immunity using bone marrow-generated dendritic cells. J Immunol 1996;156: 2918-2926.
31. Mayordomo JI, Zorina T, Storkus WJ, Zitvogel L, Celluzzi C, Falo LD Jr, et al. Bone marrow-derived dendritic cells pulsed with synthetic tumor peptide elicits protective and therapeutic antitumor immunity. Nat Med 1995;12:1297-1302.
32. Hsu FJ, Benike C, Fagnoni F, Liles TM, Czerwinski D, Taidi B, et al. Vaccination of patients with B-cell lymphoma using autologous antigen-pulsed dendritic cells. Nat Med 1996;2:52-58.
33. Nestle FO, Alijagic S, Gilliet M, Sun Y, Grabbe S, Dummer R, et al. Vaccination of melanoma patients with peptide- or tumor lysate-pulsed dendritic cells. Nat Med 1998;4:328-332.
34. Salgaller ML, Tjoa BA, Lodge PA, Ragde H, Kenny G, Boynton A, et al. Dendritic cell-based immunotherapy of prostate cancer. Crit Rev Immunol 1998;18:109-119.
35. Ferlazzo G, Munz C. NK cell compartments and their activation by dendritic cells. J Immunol 2004;172:1333-1339.
36. Zitvogel L, Mayordomo JI, Tjandrawan T, DeLeo AB, Clarke MR, Lotze MT, et al. Therapy of murine tumors with tumor peptide-pulsed dendritic cells: Dependence on T cells, B7 costimulation, and T helper cell 1-associated cytokines. J Exp Med 1996;183:87-97.

37. Osman Y, Kawamura T, Naito T, Takeda K, Van Kaer L, Okumura K, et al. Activation of hepatic NKT cells and subsequent liver injury following administration of α-galactosylceramide. Eur J Immunol 2000;30:1919-1928.
38. Fujii S, Shimizu K, Smith C, Bonifaz L, Steinman RM. Activation of natural killer T cells by α-galactosylceramide rapidly induces the full maturation of dendritic cells in vivo and thereby acts as an adjuvant for combined CD4 and CD8 T cell immunity to a coadministered protein. J Exp Med 2003;198:267-279.
39. Fujii S, Liu K, Smith C, Bonito AJ, Steinman RM. The linkage of innate to adaptive immunity via maturing dendritic cells in vivo requires CD40 ligation in addition to antigen presentation and CD80/86 costimulation. J Exp Med 2004;199:1607-1618.
40. Hermans IF, Silk JD, Gileadi U, Salio M, Mathew B, Ritter G, et al. NKT cells enhance CD4+ and CD8+ T cells responses to soluble antigen in vivo through direct interaction with dendritic cells. J Immunol 2003;171: 5140-5147.
41. Nishimura T, Kitamura H, Iwakabe K, Yahata T, Ohta A, Sato M, et al. The interface between innate and acquired immunity: glycolipid antigen presentation by CD1d-expressing dendritic cells to NKT cells induces the differentiation of antigen-specific cytotoxic T lymphocytes. Int Immunol 2000;12:987-994.

JOURNAL OF VIROLOGY, Apr. 2006, p. 3332–3340 Vol. 80, No. 7
0022-538X/06/$08.00+0 doi:10.1128/JVI.80.7.3332–3340.2006

Effect of Hepatitis C Virus (HCV) NS5B-Nucleolin Interaction on HCV Replication with HCV Subgenomic Replicon

Tetsuro Shimakami,[1] Masao Honda,[1] Takashi Kusakawa,[2] Takayuki Murata,[3] Kunitada Shimotohno,[3] Shuichi Kaneko,[1] and Seishi Murakami[2]*

Department of Gastroenterology, Kanazawa University Graduate School of Medicine,[1] and Department of Molecular Oncology, Cancer Research Institute, Kanazawa University,[2] Takara-Machi, Kanazawa, Ishikawa 920-0934, and Department of Viral Oncology, Institute for Virus Research, Kyoto University, Kawara-Cho, Sakyo-Ku, Kyoto 606-8507,[3] Japan

Received 25 September 2005/Accepted 5 January 2006

We previously reported that nucleolin, a representative nucleolar marker, interacts with nonstructural protein 5B (NS5B) of hepatitis C virus (HCV) through two independent regions of NS5B, amino acids 208 to 214 and 500 to 506. We also showed that truncated nucleolin that harbors the NS5B-binding region inhibited the RNA-dependent RNA polymerase activity of NS5B in vitro, suggesting that nucleolin may be involved in HCV replication. To address this question, we focused on NS5B amino acids 208 to 214. We constructed one alanine-substituted clustered mutant (CM) replicon, in which all the amino acids in this region were changed to alanine, as well as seven different point mutant (PM) replicons, each of which harbored an alanine substitution at one of the amino acids in the region. After transfection into Huh7 cells, the CM replicon and the PM replicon containing NS5B W208A could not replicate, whereas the remaining PM replicons were able to replicate. In vivo immunoprecipitation also showed that the W208 residue of NS5B was essential for its interaction with nucleolin, strongly suggesting that this interaction is essential for HCV replication. To gain further insight into the role of nucleolin in HCV replication, we utilized the small interfering RNA (siRNA) technique to investigate the knockdown effect of nucleolin on HCV replication. Cotransfection of replicon RNA and nucleolin siRNA into Huh7 cells moderately inhibited HCV replication, although suppression of nucleolin did not affect cell proliferation. Taken together, our findings strongly suggest that nucleolin is a host component that interacts with HCV NS5B and is indispensable for HCV replication.

Hepatitis C virus (HCV) is a major cause of chronic hepatitis around the world (1, 7). Chronic infection with HCV results in liver cirrhosis and may lead to hepatocellular carcinoma (53, 54). HCV is an enveloped positive-strand RNA virus belonging to the genus *Hepacivirus* in the family *Flaviviridae*. The HCV RNA genome is ~9.6 kb in length and consists of a 5′ nontranslated region (NTR), a large open reading frame, and a 3′ NTR. The 5′ NTR contains an internal ribosome entry site, which mediates the translation of a single polyprotein of ~3,000 amino acid (aa) residues (61, 64). This polyprotein is cleaved by host and viral proteases into at least 10 different products (33). At the amino terminus of the polyprotein are the core protein, E1, and E2, followed by p7, a hydrophobic peptide with unknown function, and the nonstructural (NS) proteins NS2, NS3, NS4A, NS4B, NS5A, and NS5B. The 3′ NTR consists of a short variable sequence, a poly(U)-poly(UC) tract, and a highly conserved X region and is critical for HCV RNA replication and HCV infection (13, 29, 69, 71).

HCV is unique among positive-strand RNA viruses in that it causes persistent and chronic infections. In addition, the high mutation rate of the gene encoding the E2 protein allows it to escape host immune surveillance, which is strongly associated with chronic inflammation of the liver (19, 23, 66, 67). As a result, HCV replication has become a target for the treatment of chronically infected individuals. The RNA-dependent RNA polymerase (RdRp) NS5B is the central catalytic enzyme in HCV RNA replication. Several recombinant and catalytically active forms of NS5B have been expressed and purified from insect cells and *Escherichia coli*, and these proteins have provided insights into the biochemical and catalytic properties of NS5B (2, 12, 34, 68). Studies of HCV replication in vitro have to overcome several difficulties, since replication requires all or most NS proteins and/or host proteins and occurs at the membrane. An understanding of the biology of HCV replication has been facilitated by the development of subgenomic and full-length HCV replicons, which express HCV proteins and replicate their RNA when transfected into human hepatoma-cell-derived Huh7 cells and other cell lines (22, 24, 35).

Nucleolin is a major nucleolar phosphoprotein, and nucleolin-specific antibodies have been used to identify nucleoli (14, 59). Nucleolin has been shown to be an RNA chaperone and/or shuttling protein for various host and viral components in nucleoli, nucleoplasm, cytoplasm, and the plasma membrane (18, 37, 41). We previously reported that the transient expression of NS5B causes the redistribution of endogenous nucleolin from the nucleus to the cytoplasm and that nucleolin and NS5B interact, in vitro and in vivo, through two independent regions of NS5B, aa 208 to 214 and 500 to 506. We also showed that the C-terminal region of nucleolin inhibited NS5B RdRp activity through this interaction in vitro (20). Because full-length nucleolin was not available in that experimental condition (70), we could not determine the exact role of this interaction in vivo.

To further investigate the interaction between nucleolin and NS5B, we focused on NS5B aa 208 to 214. We prepared a

* Corresponding author. Mailing address: Department of Molecular Oncology, Cancer Research Institute, Kanazawa University, 13-1 Takara-Machi, Kanazawa, Ishikawa, Japan. Phone: 81-76-265-2731. Fax: 81-76-234-4501. E-mail: semuraka@kenroku.kanazawa-u.ac.jp.

series of mutant replicons in which each amino acid within this region was altered to alanine(s). Here, we report that the W208 residue is critical for transient HCV replication as well as for binding to nucleolin in vivo. HCV replication was considerably inhibited in cells in which endogenous nucleolin was transiently down-regulated by small interfering RNA (siRNA). Our results strongly suggest the involvement of nucleolin in HCV replication through its interaction with NS5B and that nucleolin acts as a positive modulator of HCV replication.

MATERIALS AND METHODS

Construction of plasmids. The plasmid pNNRZ2RU (28), which harbors a subgenomic replicon derived from MT-2C cells infected with HCV (a genotype 1b isolate, M1LE [GenBank accession no. AB080299]) and contains wild-type M1LE replicon (M1LE/wild) cDNA, was digested with MluI and BglII, and the obtained fragment was inserted into the MluI and BglII sites of the vector pGL3Basic (Promega) to create pGL3-*MluI-BglII*. The intermediate vector pGL3-*MluI-BglII*-S232I was constructed by introducing the point mutation S232I of NS5A into the MluI and SacI sites of pGL3-*MluI-BglII* by site-directed mutagenesis using primers carrying the necessary nucleotide changes. Subsequently, mutations were introduced into pGL3-*MluI-BglII*-S232I, which was digested with MluI and BglII. The resulting DNA fragments were subsequently ligated into the MluI and BglII sites of pNNRZ2RU. Plasmids containing the individual NS5B substitutions W208A, K209A, S210A, K211A, K212A, C213A, and P214A and the 7-amino-acid alanine substitution, cm211, were constructed by introducing each mutation into the Eco81I and NdeI sites of pGL3-*MluI-BglII*-S232I by site-directed mutagenesis using primers carrying the necessary nucleotide changes.

The vector pNKFLAG (49) was used to express amino-terminally FLAG-tagged proteins. The plasmid pNNRZ2RU was subcloned by PCR using the primers 5′-TATCGAGCTCGATGTCAATGTCCTACTCATGGACAGGT-3′ (NS5B For), which contains an artificial initiation codon downstream of the SacI site, and 5′-ATGGATGGATCCGCGGGGTCGGGCGCGAGACAGGCT-3′ (NS5Bt Rev), which contains a BamHI site. NS5Bt, containing full-length NS5B truncated by 21 aa at the C terminus, was subcloned into the SacI and BamHI sites of pNKFLAG to create pNKFLAGNS5Bt.

The plasmid pNKGST/Nucleolin (20) was used for the expression of glutathione-*S*-transferase (GST)-fused nucleolin proteins. FLAG-labeled plasmids containing the individual NS5B substitutions W208A, K209A, S210A, K211A, K212A, C213A, and P214A and the 7-amino-acid alanine substitution cm211 were constructed by introducing fragments of pGL3-*MluI-BglII*-S232I containing each mutation into the EcoRI and SmaI sites of pNKFLAGNS5Bt.

The sequences of all the constructs were confirmed using the dideoxy sequence method. The plasmids pLMH14 and pLMH14/GHD (40) were used as templates for replicon RNA LMH14 and LMH14/GHD, respectively.

Cell culture. We used two kinds of Huh7 cells, one derived from our own laboratory's original Huh7 cells, designated Huh7-DMB (56), and the other cured of MH14 gamma interferon, designated cured MH14 (40). Huh7-DMB cells were used for colony-forming assays, and cured MH14 cells were used for luciferase assays. Both types of Huh7 cells were grown in Dulbecco's modified Eagle's medium (Gibco-BRL, Invitrogen Life Technologies) supplemented with 10% fetal bovine serum, 2 mM L-glutamine, nonessential amino acids, 100 U of penicillin, and 100 μg of streptomycin.

In vitro transcription and purification of RNA. All plasmids harboring replicon RNA were linearized with XbaI and column purified (PCR purification kit; Promega). RNA was synthesized and purified as described previously (56).

RNA transfection and selection of G418-resistant cells. Subconfluent Huh7 cells were trypsinized, washed once with phosphate-buffered saline (PBS) that does not contain Ca and Mg [PBS(−)], and resuspended at 10^7 cells/ml in OPTI-MEM (Gibco-BRL, Invitrogen Life Technologies). One hundred nanograms of *neo* replicon RNA, with or without 1 μM of each siRNA, was added to 400 μl of each cell suspension in a cuvette with a gap width of 0.4 cm (Bio-Rad). The mixture was immediately transfected into Huh7 cells by electroporation with a GenePulser II system (Bio-Rad) set to 270 V and 975 μF. Following a 10-min incubation at room temperature, the cells were transferred into 10 ml of growth medium and seeded into a 10-cm-diameter cell culture dish. To select G418-resistant cells, the medium was replaced with fresh medium containing 1 mg/ml of G418 (GENETICIN; Gibco-BRL, Invitrogen Life Technologies) 24 h after transfection. After changing the medium twice per week for 4 weeks, the colonies were stained with Coomassie brilliant blue (0.6 g/liter in 50% methanol–10% acetic acid).

DNA transfection. Using the same electroporation protocol as described above, 500 ng of pCI-Neo (Promega), which encodes a neomycin resistance marker under the control of a cytomegalovirus (CMV) promoter/enhancer, with or without 1 μM of each siRNA, was transfected into Huh7 cells. G418-resistant cells were selected in medium containing 0.5 mg/ml G418. Four weeks after transfection, the colonies were stained with Coomassie brilliant blue.

Using DMRIE-C reagent (Invitrogen Life Technologies), 300 ng of pGL3 control (Promega), encoding luciferase under the control of a CMV promoter/enhancer, was cotransfected with or without 2 μM of each siRNA according to the manufacturer's instructions. Luciferase activity was assayed 48 and 72 h after transfection.

RNA transfection and luciferase assay. We used a luciferase assay to monitor luciferase replicon activity. Briefly, cured MH14 cells seeded onto 48-well plates were transfected with 250 ng of luciferase replicon RNA, with or without 2 μM of each siRNA, using DMRIE-C reagent according to the manufacturer's instructions. Cell proteins were extracted in a lysis buffer supplied in the Dual-Luciferase Reporter Assay system (Promega), and their luciferase activity was measured. Each assay was performed at least in triplicate, and means and standard deviations were determined.

Preparation of cell extracts, coprecipitation with glutathione resin, and Western blot analysis. COS1 cells were transiently transfected using the calcium-phosphate method. The cells were harvested, washed with PBS(−), and sonicated in PBS lysis buffer [PBS(−) containing 150 mM NaCl, 1.0% Triton X-100, 1 mM EDTA, and 1 mM dithiothreitol] containing 10 μg each of aprotinin and leupeptin per ml. Total cell lysates were diluted 10-fold with PBS lysis buffer, mixed with 20 μl of glutathione-Sepharose 4B beads (glutathione resin) (Amersham Biosciences), and incubated for 3 h on a rotator in a cold room. After extensive washing with PBS(−) containing 1.0% Triton X-100, the bound proteins were eluted, fractionated by sodium dodecyl sulfate (SDS)–10% polyacrylamide gel electrophoresis (PAGE), transferred onto nitrocellulose membranes, and subjected to Western blot analysis with anti-FLAG M2 monoclonal antibody (Sigma). The proteins were visualized using enhanced chemiluminescence according to the manufacturer's instructions (Amersham Biosciences). As a loading control, the nitrocellulose membranes used for Western blot analysis with anti-FLAG M2 monoclonal antibody were reprobed with anti-GST monoclonal antibody (Santa Cruz Biotechnology, Inc.) according to the manufacturer's instructions (Amersham Biosciences).

siRNA. We purchased siRNA for luciferase GL3 duplex (si-Luc), siRNA for nonspecific control RNA duplex (si-Mix), siRNA for nucleolin (si-Nuc) (GGA AGACGGUGAAAUUGAU-deoxyribosylthymine [dT]dT), and siRNA for HCV (CCUCAAAGAAAAACCAAAC-dTdT) from B-Bridge International, Inc., and we purchased siRNA for GFP from QIAGEN.

Western blot analysis for endogenous nucleolin. Using the electroporation protocol described above, 1 μM of each siRNA was transfected into Huh7-DMB cells. After 48 h, the cells were harvested, washed with PBS(−), and sonicated in PBS lysis buffer. Total cell lysates were fractionated by SDS–10% PAGE, transferred onto nitrocellulose membranes, and subjected to Western blot analysis with rabbit polyclonal anti-nucleolin antibody (103C) (20), mouse monoclonal anti-nucleolin antibody (C23, sc-8031; Santa Cruz Biotechnology, Inc.), and mouse monoclonal anti-β-actin antibody (Sigma). The proteins were visualized by enhanced chemiluminescence according to the manufacturer's instructions (Amersham Biosciences).

RESULTS

We previously reported that NS5B from HCV subtype 1b isolate JK-1 and nucleolin interact in vitro and in vivo and that two regions of NS5B, amino acids 208 to 214 and 500 to 506, are both indispensable for binding to nucleolin. We also reported that the C-terminal region of nucleolin inhibited the RdRp activity of NS5B in a dose-dependent manner (20). Although the effect of full-length nucleolin could not be determined, because we could not obtain recombinant full-length nucleolin, these results strongly suggested that nucleolin may be a component of the HCV replication complex and, through its interaction with NS5B, may modulate HCV replication. To further investigate this question, we determined the biological effect of the interaction between NS5B from HCV subtype 1b

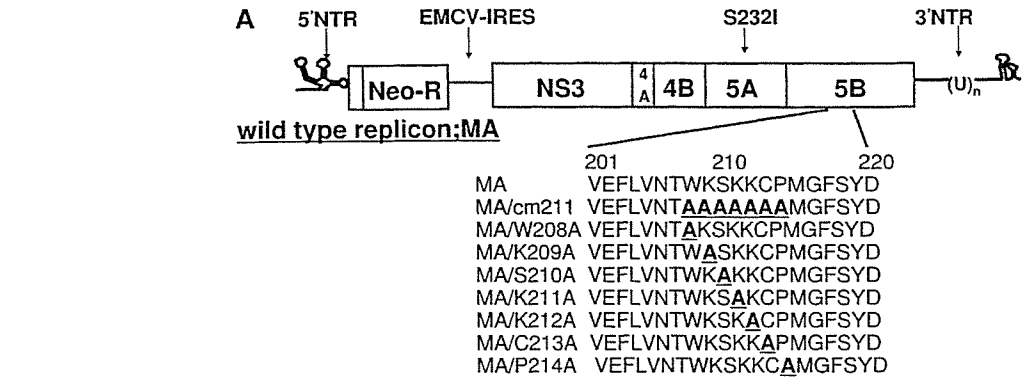

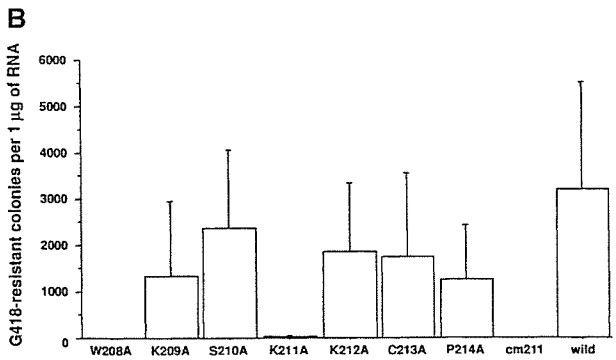

FIG. 1. (A) Schematic representation of the mutant replicons used in this study. MA is a replicon carrying the point mutation S232I in NS5A and was used as the wild-type replicon. The mutant replicons MA/cm211, MA/W208A, MA/209A, MA/S210A, MA/211A, MA/212A, MA/213A, and MA/214A carry NS5B mutations in MA, as shown. Numbering starts from the beginning of NS5B. EMCV, encephalomyocarditis virus; IRES, internal ribosome entry site. (B) Effect of each mutation on HCV RNA replication. Huh7-DMB cells were electroporated with 1 μg of each replicon RNA, and G418-resistant cells were selected with 1 mg/ml G418 and stained 4 weeks later. This figure shows the mean number of G418-resistant cell colonies per 10-cm-diameter cell culture dish per 1 μg replicon RNA.

isolate M1LE and nucleolin on HCV replication using an HCV subgenomic replicon system.

Scanning of aa 208 to 214 in an HCV subgenomic replicon. First, we tested the importance of NS5B aa 208 to 214, a region essential for nucleolin binding, in HCV RNA replication. For this purpose, we prepared eight mutant replicons (Fig. 1A). The wild-type replicon was represented by MA, in which S232 of NS5A was altered to I, because this mutant replicon can efficiently replicate in Huh7 cells (36, 56). In the replicon MA/cm211, each of the amino acids at positions 208 to 214 of NS5B was changed to alanine, whereas in the replicons MA/W208A, K209A, S210A, K211A, K212A, C213A, and P214A, each individual amino acid residue was changed to alanine. All of these mutant replicons were transfected into Huh7-DMB cells, which were selected with G418, and the number of G418-resistant colonies was used as an indication of HCV RNA replication. In cells transfected with MA/cm211 and MA/W208A, we observed no G418-resistant colonies, whereas in cells transfected with the six other point mutant replicons, as well as in cells transfected with MA/K211, we detected G418-resistant colonies, but they were fewer than those detected with wild-type replicon MA (Fig. 1B). Our negative control, the mutant replicon M1LE/5B-VDD, in which the GDD motif of NS5B was mutated to VDD, yielded no G418-resistant colonies (data not shown). The results of this experiment indicated that the region of NS5B at aa 208 to 214, especially W208, is essential for HCV RNA replication.

Interaction between nucleolin and NS5B. Although we have shown that NS5B from isolate JK-1 binds to nucleolin, it was necessary to show this in isolate M1LE. Due to the poor recovery of soluble full-length NS5B, we utilized NS5Bt (68), a soluble form of NS5B in which the C-terminal 21 aa were truncated, to dissect the interaction between NS5B and nucleolin. Previously, we confirmed that these 21 deleted amino acids were not essential for this interaction (20). FLAG-NS5Bt and GST-nucleolin were transiently coexpressed in COS1 cells, after which the lysates were subjected to a GST pull-down assay and the bound proteins were immunologically detected with anti-FLAG M2 and anti-GST antibodies. We found that GST-nucleolin could bind FLAG-NS5Bt from the M1LE isolate, whereas GST could not, indicating that nucleolin interacts with NS5B in both JK-1 and M1LE isolates (Fig. 2). To determine the essential region/residues of NS5B required for its binding to nucleolin, we again focused on aa 208 to 214 using the alanine scanning method (3). We prepared FLAG-NS5Bt/cm211, in which aa 208 to 214 were all replaced by alanine residues, and showed that it could not bind to GST-nucleolin in an in vivo immunoprecipitation assay (Fig. 2), indicating that aa 208 to 214 of NS5B in both M1LE and JK-1 isolates constitute a critical region for the binding of nucleolin. To identify the exact residue(s) within aa 208 to 214 critical for binding to nucleolin, we prepared seven alanine-substituted point mutants in which each amino acid was replaced by alanine, and we tested the ability of each point mutant to bind to GST-nucleolin. Using an in vivo immunoprecipitation assay, we found that of the seven point mutants, only FLAG-NS5Bt/W208A could not bind to GST-nucleolin (Fig. 2), indicating that W208 of NS5B is essential for this binding and may be essential for HCV replication.

Suppression of endogenous nucleolin by siRNA. To identify the siRNA sequence that knocks down the expression of endogenous nucleolin, we used the prediction services of

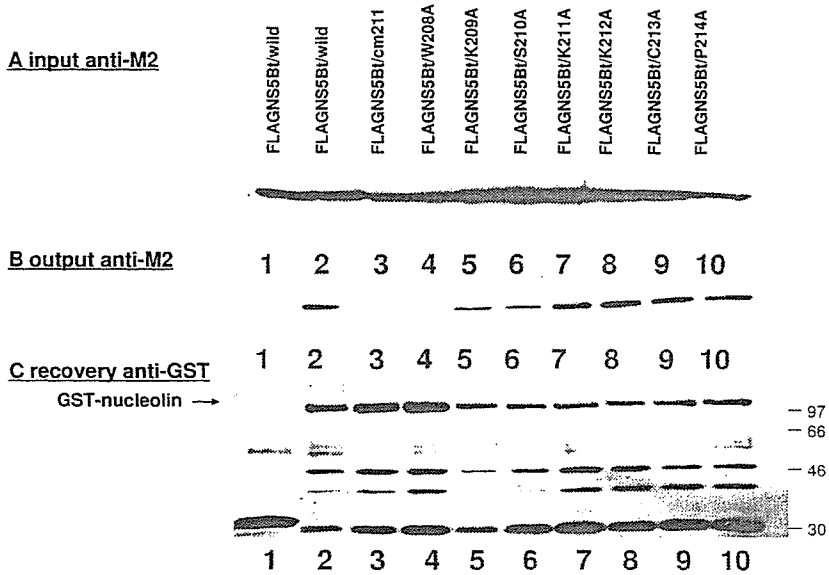

FIG. 2. Interaction between nucleolin and NS5B of HCV isolate M1LE and an essential residue for this interaction. COS1 cells were transiently cotransfected with mammalian expression vectors expressing FLAG-NS5Bt proteins (lanes: 1 and 2, wild type; 3, cm211; 4, W208A; 5, K209A; 6, S210A; 7, K211A; 8, K212A; 9, C213A; 10, P214A) and GST protein alone (lane 1) or GST-nucleolin protein (lanes 2 to 10). (A) Input of FLAG-NS5Bt proteins. Total lysates were fractionated by SDS–10% PAGE and subjected to Western blot analysis with anti-FLAG M2 monoclonal antibody. (B) Output of FLAG-NS5Bt proteins. Coprecipitants by glutathione resin were washed with PBS(−) containing 1.0% Triton X-100, fractionated by SDS–10% PAGE, and subjected to Western blot analysis with anti-FLAG M2 monoclonal antibody. (C) Recovery of GST or GST-nucleolin proteins. The nitrocellulose membrane used for Western blot analysis of coprecipitants with anti-FLAG M2 antibody was reprobed with anti-GST antibody. Molecular masses (kilodaltons) are indicated to the right of the panel.

iGENE (Tsukuba, Japan). We selected one sequence, si-Nuc, and, as a control for siRNA transfection, we utilized siRNA for luciferase (si-Luc) (GL3 luciferase duplex). Forty-eight hours after electroporation of each siRNA, at a concentration of 1 μM, into Huh7-DMB, the lysates were analyzed by Western blotting analysis with two kinds of antibody to nucleolin. We found that both anti-nucleolin antibodies detected the expression of endogenous nucleolin. Although si-Nuc efficiently knocked down the expression of endogenous nucleolin, si-Luc did not (Fig. 3), showing the specificity of the former. In addition, real-time PCR showed that si-Nuc decreased nucleolin mRNA by about one-third compared with si-Luc (data not shown).

Effect of nucleolin suppression on HCV replication. To test the effect of nucleolin knockdown on HCV RNA replication, we transfected 1 μM of si-Nuc or si-Luc along with 100 ng of replicon MA RNA into Huh7-DMB cells and selected the cells with G418. As shown in Fig. 4, we found that cotransfection of si-Nuc reduced the number of G418-resistant colonies, whereas cotransfection of si-Luc did not (Fig. 4). As a control for the efficient transfection of siRNA, we used si-HCV, which targets the HCV internal ribosome entry site and can efficiently suppress HCV replication, as described previously (51). Using this siRNA, we observed no G418-resistant colonies, indicating that siRNA was efficiently transfected under these experimental conditions. To rule out the possibility that suppression of nucleolin may have a detrimental effect on cells and may inhibit HCV RNA replication, we transfected pCI-Neo, which encodes a neomycin resistance gene under the control of a CMV promoter/enhancer, into Huh7-DMB cells, with or without si-Nuc and si-Luc, and selected the cells with 0.5 mg/dl G418. We found that the suppression of nucleolin expression did not significantly reduce the number of G418-resistant colonies (data not shown). In addition, massive cell death was not observed after the transfection of any siRNA (data not shown). These results indicate that the transient suppression of nucleolin may not affect cell proliferation but that nucleolin may affect the HCV replication complex itself.

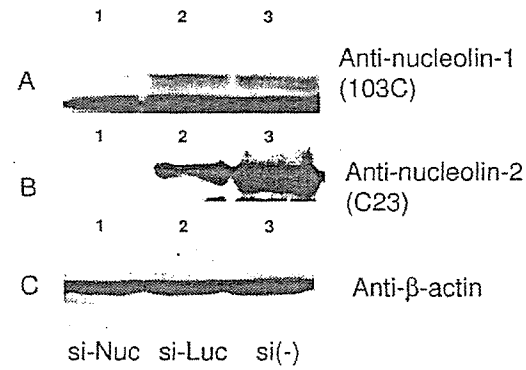

FIG. 3. Knockdown of endogenous nucleolin by siRNA. Huh7-DMB cells were electroporated with 1 μM si-Nuc and si-Luc. After 48 h, total cell lysates were fractionated by SDS–10% PAGE and subjected to Western blot analysis with the anti-nucleolin antibodies anti-nucleolin-1 (103C) in A and anti-nucleolin-2 (C23) in B and anti-β-actin antibody in C. Lanes: 1, cells transfected with si-Nuc; 2, cells transfected with si-Luc; 3, no siRNA [si(−)].

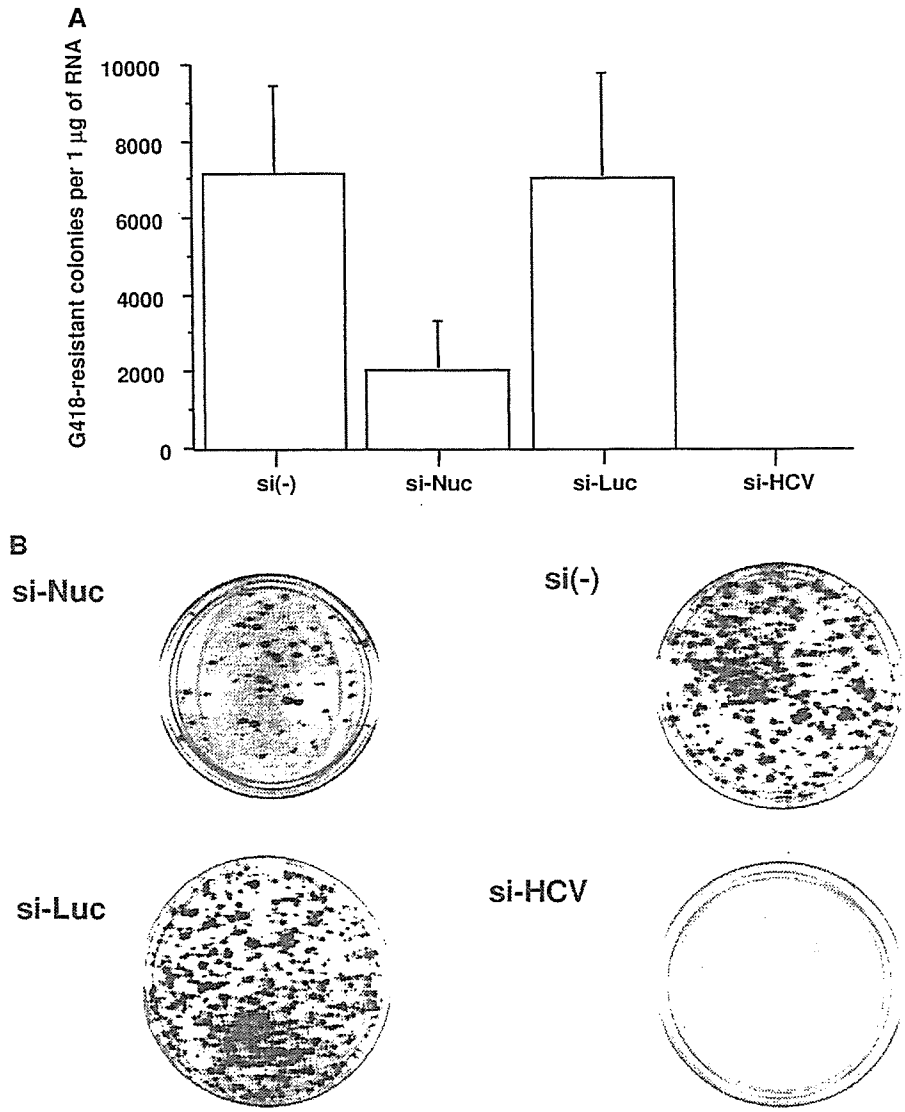

FIG. 4. Effect of suppression of endogenous nucleolin on HCV replication in the MA replicon. Huh7-DMB cells were electroporated with 1 μg of in vitro-transcribed MA RNA plus si-Nuc, si-Luc, si-HCV, or no siRNA [si(−)], and G418-resistant cells were selected with 1 mg/ml G418 and were stained 4 weeks later. (A) Mean number of G418-resistant colonies per 10-cm-diameter cell culture dish per 1 μg replicon RNA. Error bars indicate the standard deviations of the results from at least three independent experiments. (B) Visualization of G418-resistant colonies, as described in Materials and Methods.

Because the knockdown effect of siRNA does not continue for more than 3 weeks after transient transfection, the number of G418-resistant colonies may not be a good indicator of HCV RNA replication. We therefore performed a transient replication assay using a replicon in which the neomycin resistance gene was replaced by a luciferase gene, and luciferase activity was used as a marker of HCV RNA replication. Transfection of MH14 RNA, which was used as the wild-type replicon, into a subline of Huh7 cells resulted in highly efficient luciferase activity, whereas a polymerase-defective RNA replicon of MH14, MH4GHD, in which the catalytic GDD motif of NS5B polymerase was replaced by an inactive GHD motif, was used as a negative control (Fig. 5A). si-HCV and si-Luc suppressed the luciferase activity even at 24 h after transfection, but other siRNAs did not affect the luciferase activity, and luciferase activities in these siRNAs were similar to that of the control (no siRNA) at this point (Fig. 5B). We found that cotransfection of si-Nuc moderately suppressed both luciferase activity at 72 h after transfection and relative luciferase activity, whereas cotransfection of si-GFP and si-Mix did not (Fig. 5B and C). Cotransfection of si-HCV and si-Luc almost completely suppressed luciferase activity at 72 h after transfection. In a transient replication assay, the suppression of endogenous nucleolin also inhibited HCV replication.

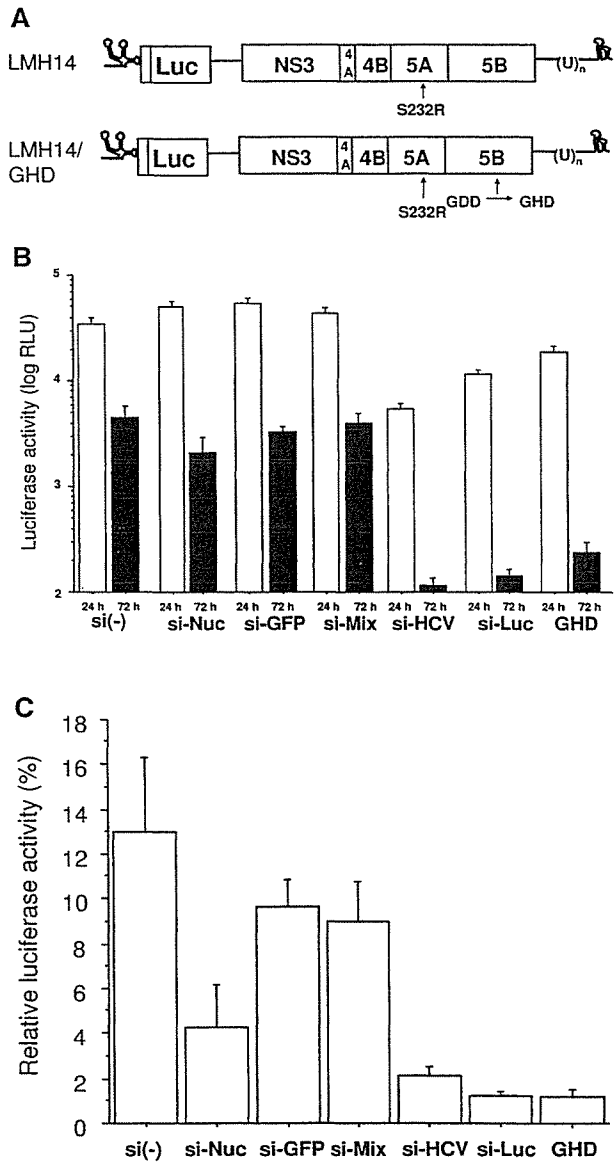

FIG. 5. Effect of suppression of endogenous nucleolin on HCV replication in the LMH14 replicon. (A) Schematic representation of the luciferase replicon. In the LMH14 replicon, the neomycin resistance gene was replaced by a luciferase gene, and S232 of NS5A was replaced by R. In the LMH14/GHD replicon, the NS5B GDD motif in LMH14 was changed to GHD and used as a negative control. (B) Cells were transfected with in vitro-transcribed LHH14 or LMH14/GHD RNA along with 2 μM of si-Mix, si-GFP, si-Nuc, si-Luc, si-HCV, or no siRNA [si(−)] using the DMRIE-C reagent, and luciferase activity (relative light units [RLU]) was measured 24 and 72 h after transfection. Shown are the activities at 24 and 72 h. Error bars indicate the standard deviations of the results from at least three independent experiments. (C) Activity at 24 h was used as an indication of each transfection. Shown are the ratios of activity (percent) at 72 h relative to that at 24 h. Error bars indicate the standard deviations of the results from at least three independent experiments.

To rule out the cytotoxic effects of the suppression of endogenous nucleolin, we transfected pGL3 control, with or without each siRNA, and measured luciferase activity 48 and 72 h after transfection. We found that cotransfection of each siRNA did not inhibit luciferase activity at both 48 and 72 h (Fig. 6), indicating that both suppression of nucleolin and transfection of siRNA did not have detrimental effects on transfected cells.

DISCUSSION

HCV replication has been found to take place in a distinctly altered membrane structure, or membranous web, of the endoplasmic reticulum (11). When HCV NS proteins are coexpressed in stable cell lines harboring replicons, they colocalize to these membrane structures, indicating that they might form a complex (16, 39, 47). These nonstructural proteins, together with host factors, form the viral replicase, the complex in which viral replication is thought to take place. The in vitro level of the RdRp activity of NS5B is low (12), indicating that cofactors, whether viral and/or host proteins and/or the appropriate cellular environment, are necessary for optimal activity of HCV RdRp. HCV NS5B has been reported to interact with NS3, NS4A, NS4B, NS5A, and NS5B itself (9, 48, 57, 65). Using an HCV subgenomic replicon, we previously reported the critical role of the interaction between NS5A and NS5B and the oligomerization of NS5B itself in HCV replication (36, 56). NS3 and NS4B have been shown to be positive and negative regulators, respectively, of NS5B in the replication complex (46).

In addition to interacting with HCV nonstructural proteins, NS5B has been reported to interact with many host proteins, including a SNARE-like protein (62); eIF4AII, an RNA-dependent ATPase/helicase; a component of the translation initiation complex (30), protein kinase C-related kinase 2, which specifically phosphorylates NS5B (27); and p68, a human RNA helicase I (15). The suppression of protein kinase C-related kinase 2 has been reported to reduce the phosphorylation of NS5B and to inhibit HCV RNA replication (27), and the suppression of p68 has been reported to inhibit the synthesis of negative-strand HCV RNA from the positive strand (15).

Several host proteins have been shown to interact with RdRp of other RNA viruses. For example, in poliovirus, an RdRp and an RdRp precursor interact with human Sam68 (38) and heterogeneous nuclear ribonucleoprotein C1/C2 (5), respectively, and modulate RdRp activity directly or indirectly. Bromo mosaic virus RdRp and tobacco mosaic virus RdRp interact with eukaryotic initiation factor 3 and eukaryotic initiation factor 3-related factor, altering RdRp activity (45, 50).

Here and in a previous report, we identified and characterized the interaction between nucleolin and HCV NS5B (20). Nucleolin was originally identified as a common phosphoprotein of growing eukaryotic cells, although its function is not completely understood. Nucleolin is a multifunctional protein that shuttles between the nucleus and cytoplasm. In addition, it is expressed on the surface of various cells, acting as a receptor for various ligands, including lipoproteins (55), cytokines, growth factors (6, 52, 60), the extracellular matrix (10, 18, 25), bacteria (58), and viruses (4, 8, 21, 41–44).

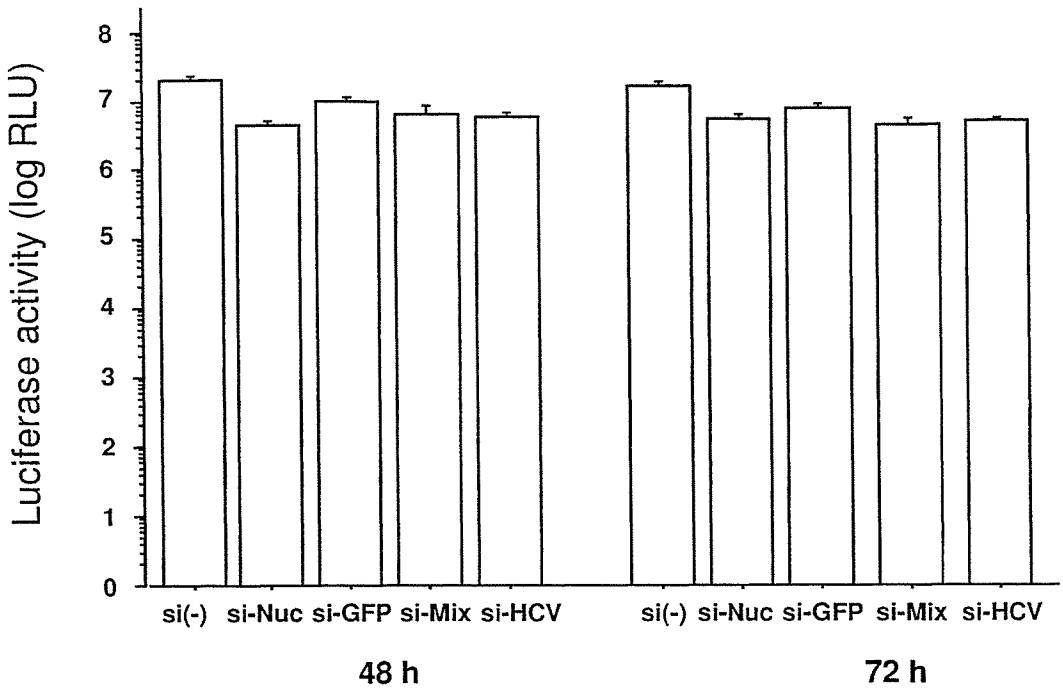

FIG. 6. Effect of suppression of endogenous nucleolin on cell proliferation. The plasmid pGL3 control, encoding the luciferase gene under the control of the CMV promoter/enhancer, was cotransfected with 2 μM of si-Mix, si-GFP, si-Nuc, si-HCV, or no siRNA [si(−)] using DMRIE-C reagent, and luciferase activity was measured 48 and 72 h after transfection. The error bars indicate the standard deviations of the results from at least three independent experiments.

We found that recombinant C-terminal nucleolin proteins can bind NS5B and inhibit its RdRp activity in a dose-dependent manner (20), suggesting that nucleolin may affect HCV replication by interacting with NS5B. The direct interaction of nucleolin with HCV NS5B in vivo and in vitro was shown to require two critical stretches of NS5B. Here, we showed that within one of these regions, aa 208 to 214, the W208 residue was critical for both binding of nucleolin and HCV replication. Transient down-regulation of endogenous nucleolin by siRNA considerably inhibited HCV replication in Huh7 cells. These results strongly indicate that nucleolin has an important role in HCV replication through its direct interaction with NS5B.

Our finding of an important positive role for nucleolin in HCV replication is apparently inconsistent with previous findings of an inhibitory role for nucleolin. It was previously reported that purified C-terminal nucleolin proteins inhibited the RdRp activity of NS5B in vitro. The latter result, however, may have been due to the use of recombinant truncated nucleolin proteins, because recombinant full-length nucleolin was not available (70). Taken together, however, these results indicate that N-terminal nucleolin may be important for the positive function of nucleolin in HCV replication, although the NS5B-binding region is within the RGG domain and RNA-binding domain 4 is at the C terminus.

Transfection of the mutant replicon containing NS5B W208A, which could not bind nucleolin, led to almost no HCV replication. By contrast, the suppression of nucleolin by siRNA moderately inhibited HCV replication, a result also observed with the transient assay using luciferase reporter replicon and G418-resistant colony formation. While HCV replication was completely inhibited by MA/W208A, replication was only partially inhibited by si-Nuc, indicating that si-Nuc can transiently suppress, but cannot eliminate, expression of endogenous nucleolin. Recently, nucleolin was reported to inhibit cell cycle progression after heat shock and genotoxic stress by increasing complex formation with human replication protein A (26). When pGL3 control or pCI-Neo was cotransfected with si-Nuc, the luciferase activity or the number of G418-resistant colonies was not reduced, strongly suggesting that the moderate inhibition of nucleolin expression did not have severe cytotoxic effects on siRNA-transfected cells. More efficient suppression of nucleolin may result in more severe inhibition of HCV RNA replication. It is therefore important to determine whether nucleolin is dispensable in mammalian cells as it is in *Saccharomyces pombe* (17) and *Saccharomyces cerevisiae* (31), since nucleolin may constitute a putative therapeutic target to inhibit HCV replication.

Using a clustered alanine substitution mutant library (CM) of NS5B, we previously showed that two stretches of NS5B amino acids, aa 208 to 214 and 500 to 506, were critical for nucleolin binding. According to the crystal models of NS5B, the former stretch is in the palm and the latter stretch is in the bottom of the thumb domain. We focused on identifying residues in aa 208 to 214 that are essential for nucleolin binding and HCV replication, as the CM mutant of aa 500 to 506 was defective in RdRp activity in vitro and HCV replication in vivo (36, 48, 49). We found that the W208 residue was critical for

both nucleolin binding and HCV replication. This residue is exposed to solvent at the edge of the palm and is not close to the catalytic pocket.

Nucleolin may stabilize monomeric NS5B, making it ready for oligomerization to NS5B, or it may facilitate the formation of a complex between NS5B and template RNA. In both cases, a substoichiometric amount of nucleolin may be required transiently at a step prior to the catalytic RdRp reaction of NS5B. Efforts to determine the contribution of amino acid residues 500 to 508 to nucleolin binding and HCV replication in vivo are ongoing and may reveal further correlations. We found that another mutant replicon, MA/K211A, reduced the number of G418-resistant colonies compared with the wild type and the other mutants. Because K211A of NS5Bt is close to the pocket of catalytic activity and did not affect binding to nucleolin, K211 may contribute to the structural integrity of the pocket or the heat-stable property of RdRp as reported previously (36).

Efficient HCV replication and infection in tissue-cultured cells by using full-length HCV RNA replicons have been reported previously (32, 63, 72). HCV replication occurs in differentiated subcellular fractions and involves dynamic complexes of structural proteins, nonstructural proteins, and HCV RNA demarcated by membrane structures. It is therefore of great interest to determine whether nucleolin is involved in such HCV-replicating intermediates in compartmented subcellular structures.

REFERENCES

1. **Alter, H. J., R. H. Purcell, J. W. Shih, J. C. Melpolder, M. Houghton, Q. L. Choo, and G. Kuo.** 1989. Detection of antibody to hepatitis C virus in prospectively followed transfusion recipients with acute and chronic non-A, non-B hepatitis. N. Engl. J. Med. **321**:1494–1500.
2. **Behrens, S. E., L. Tomei, and R. De Francesco.** 1996. Identification and properties of the RNA-dependent RNA polymerase of hepatitis C virus. EMBO J. **15**:12–22.
3. **Bordo, D., and P. Argos.** 1991. Suggestions for "safe" residue substitutions in site-directed mutagenesis. J. Mol. Biol. **217**:721–729.
4. **Bose, S., M. Basu, and A. K. Banerjee.** 2004. Role of nucleolin in human parainfluenza virus type 3 infection of human lung epithelial cells. J. Virol. **78**:8146–8158.
5. **Brunner, J. E., J. H. Nguyen, H. H. Roehl, T. V. Ho, K. M. Swiderek, and B. L. Semler.** 2005. Functional interaction of heterogeneous nuclear ribonucleoprotein C with poliovirus RNA synthesis initiation complexes. J. Virol. **79**:3254–3266.
6. **Callebaut, C., S. Nisole, J. P. Briand, B. Krust, and A. G. Hovanessian.** 2001. Inhibition of HIV infection by the cytokine midkine. Virology **281**:248–264.
7. **Choo, Q. L., G. Kuo, A. J. Weiner, L. R. Overby, D. W. Bradley, and M. Houghton.** 1989. Isolation of a cDNA clone derived from a blood-borne non-A, non-B viral hepatitis genome. Science **244**:359–362.
8. **de Verdugo, U. R., H. C. Selinka, M. Huber, B. Kramer, J. Kellermann, P. H. Hofschneider, and R. Kandolf.** 1995. Characterization of a 100-kilodalton binding protein for the six serotypes of coxsackie B viruses. J. Virol. **69**:6751–6757.
9. **Dimitrova, M., I. Imbert, M. P. Kieny, and C. Schuster.** 2003. Protein-protein interactions between hepatitis C virus nonstructural proteins. J. Virol. **77**:5401–5414.
10. **Dumler, I., V. Stepanova, U. Jerke, O. A. Mayboroda, F. Vogel, P. Bouvet, V. Tkachuk, H. Haller, and D. C. Gulba.** 1999. Urokinase-induced mitogenesis is mediated by casein kinase 2 and nucleolin. Curr. Biol. **9**:1468–1476.
11. **Egger, D., B. Wolk, R. Gosert, L. Bianchi, H. E. Blum, D. Moradpour, and K. Bienz.** 2002. Expression of hepatitis C virus proteins induces distinct membrane alterations including a candidate viral replication complex. J. Virol. **76**:5974–5984.
12. **Ferrari, E., J. Wright-Minogue, J. W. Fang, B. M. Baroudy, J. Y. Lau, and Z. Hong.** 1999. Characterization of soluble hepatitis C virus RNA-dependent RNA polymerase expressed in *Escherichia coli*. J. Virol. **73**:1649–1654.
13. **Friebe, P., and R. Bartenschlager.** 2002. Genetic analysis of sequences in the 3′ nontranslated region of hepatitis C virus that are important for RNA replication. J. Virol. **76**:5326–5338.
14. **Ginisty, H., H. Sicard, B. Roger, and P. Bouvet.** 1999. Structure and functions of nucleolin. J. Cell Sci. **112**:761–772.
15. **Goh, P. Y., Y. J. Tan, S. P. Lim, Y. H. Tan, S. G. Lim, F. Fuller-Pace, and W. Hong.** 2004. Cellular RNA helicase p68 relocalization and interaction with the hepatitis C virus (HCV) NS5B protein and the potential role of p68 in HCV RNA replication. J. Virol. **78**:5288–5298.
16. **Gosert, R., D. Egger, V. Lohmann, R. Bartenschlager, H. E. Blum, K. Bienz, and D. Moradpour.** 2003. Identification of the hepatitis C virus RNA replication complex in Huh-7 cells harboring subgenomic replicons. J. Virol. **77**:5487–5492.
17. **Gulli, M. P., J. P. Girard, D. Zabetakis, B. Lapeyre, T. Melese, and M. Caizergues-Ferrer.** 1995. gar2 is a nucleolar protein from Schizosaccharomyces pombe required for 18S rRNA and 40S ribosomal subunit accumulation. Nucleic Acids Res. **23**:1912–1918.
18. **Harms, G., R. Kraft, G. Grelle, B. Volz, J. Dernedde, and R. Tauber.** 2001. Identification of nucleolin as a new L-selectin ligand. Biochem. J. **360**:531–538.
19. **Hijikata, M., N. Kato, Y. Ootsuyama, M. Nakagawa, S. Ohkoshi, and K. Shimotohno.** 1991. Hypervariable regions in the putative glycoprotein of hepatitis C virus. Biochem. Biophys. Res. Commun. **175**:220–228.
20. **Hirano, M., S. Kaneko, T. Yamashita, H. Luo, W. Qin, Y. Shirota, T. Nomura, K. Kobayashi, and S. Murakami.** 2003. Direct interaction between nucleolin and hepatitis C virus NS5B. J. Biol. Chem. **278**:5109–5115.
21. **Hovanessian, A. G., F. Puvion-Dutilleul, S. Nisole, J. Svab, E. Perret, J. S. Deng, and B. Krust.** 2000. The cell-surface-expressed nucleolin is associated with the actin cytoskeleton. Exp. Cell Res. **261**:312–328.
22. **Ikeda, M., M. Yi, K. Li, and S. M. Lemon.** 2002. Selectable subgenomic and genome-length dicistronic RNAs derived from an infectious molecular clone of the HCV-N strain of hepatitis C virus replicate efficiently in cultured Huh7 cells. J. Virol. **76**:2997–3006.
23. **Kato, N., Y. Ootsuyama, H. Sekiya, S. Ohkoshi, T. Nakazawa, M. Hijikata, and K. Shimotohno.** 1994. Genetic drift in hypervariable region 1 of the viral genome in persistent hepatitis C virus infection. J. Virol. **68**:4776–4784.
24. **Kato, T., T. Date, M. Miyamoto, Z. Zhao, M. Mizokami, and T. Wakita.** 2005. Nonhepatic cell lines HeLa and 293 support efficient replication of the hepatitis C virus genotype 2a subgenomic replicon. J. Virol. **79**:592–596.
25. **Kibbey, M. C., B. Johnson, R. Petryshyn, M. Jucker, and H. K. Kleinman.** 1995. A 110-kD nuclear shuttling protein, nucleolin, binds to the neurite-promoting IKVAV site of laminin-1. J. Neurosci. Res. **42**:314–322.
26. **Kim, K., D. D. Dimitrova, K. M. Carta, A. Saxena, M. Daras, and J. A. Borowiec.** 2005. Novel checkpoint response to genotoxic stress mediated by nucleolin-replication protein A complex formation. Mol. Cell. Biol. **25**:2463–2474.
27. **Kim, S. J., J. H. Kim, Y. G. Kim, H. S. Lim, and J. W. Oh.** 2004. Protein kinase C-related kinase 2 regulates hepatitis C virus RNA polymerase function by phosphorylation. J. Biol. Chem. **279**:50031–50041.
28. **Kishine, H., K. Sugiyama, M. Hijikata, N. Kato, H. Takahashi, T. Noshi, Y. Nio, M. Hosaka, Y. Miyanari, and K. Shimotohno.** 2002. Subgenomic replicon derived from a cell line infected with the hepatitis C virus. Biochem. Biophys. Res. Commun. **293**:993–999.
29. **Kolykhalov, A. A., K. Mihalik, S. M. Feinstone, and C. M. Rice.** 2000. Hepatitis C virus-encoded enzymatic activities and conserved RNA elements in the 3′ nontranslated region are essential for virus replication in vivo. J. Virol. **74**:2046–2051.
30. **Kyono, K., M. Miyashiro, and I. Taguchi.** 2002. Human eukaryotic initiation factor 4AII associates with hepatitis C virus NS5B protein *in vitro*. Biochem. Biophys. Res. Commun. **292**:659–666.
31. **Lee, W. C., D. Zabetakis, and T. Melese.** 1992. NSR1 is required for pre-rRNA processing and for the proper maintenance of steady-state levels of ribosomal subunits. Mol. Cell. Biol. **12**:3865–3871.
32. **Lindenbach, B. D., M. J. Evans, A. J. Syder, B. Wolk, T. L. Tellinghuisen, C. C. Liu, T. Maruyama, R. O. Hynes, D. R. Burton, J. A. McKeating, and C. M. Rice.** 2005. Complete replication of hepatitis C virus in cell culture. Science **309**:623–626.
33. **Lindenbach, B. D., and C. M. Rice.** 2005. Unravelling hepatitis C virus replication from genome to function. Nature **436**:933–938.
34. **Lohmann, V., F. Korner, U. Herian, and R. Bartenschlager.** 1997. Biochemical properties of hepatitis C virus NS5B RNA-dependent RNA polymerase and identification of amino acid sequence motifs essential for enzymatic activity. J. Virol. **71**:8416–8428.
35. **Lohmann, V., F. Korner, J. Koch, U. Herian, L. Theilmann, and R. Bartenschlager.** 1999. Replication of subgenomic hepatitis C virus RNAs in a hepatoma cell line. Science **285**:110–113.
36. **Ma, Y., T. Shimakami, H. Luo, N. Hayashi, and S. Murakami.** 2004. Mutational analysis of hepatitis C virus NS5B in the subgenomic replicon cell culture. J. Biol. Chem. **279**:25474–25482.
37. **Matthews, D. A.** 2001. Adenovirus protein V induces redistribution of nucleolin and B23 from nucleolus to cytoplasm. J. Virol. **75**:1031–1038.
38. **McBride, A. E., A. Schlegel, and K. Kirkegaard.** 1996. Human protein Sam68 relocalization and interaction with poliovirus RNA polymerase in infected cells. Proc. Natl. Acad. Sci. USA **93**:2296–2301.
39. **Mottola, G., G. Cardinali, A. Ceccacci, C. Trozzi, L. Bartholomew, M. R. Torrisi, E. Pedrazzini, S. Bonatti, and G. Migliaccio.** 2002. Hepatitis C virus

nonstructural proteins are localized in a modified endoplasmic reticulum of cells expressing viral subgenomic replicons. Virology 293:31–43.
40. **Murata, T., T. Obshima, M. Yamaji, M. Hosaka, Y. Miyanari, M. Hijikata, and K. Shimotohno.** 2005. Suppression of hepatitis C virus replicon by TGF-beta. Virology 331:407–417.
41. **Nisole, S., B. Krust, C. Callebaut, G. Guichard, S. Muller, J. P. Briand, and A. G. Hovanessian.** 1999. The anti-HIV pseudopeptide HB-19 forms a complex with the cell-surface-expressed nucleolin independent of heparan sulfate proteoglycans. J. Biol. Chem. 274:27875–27884.
42. **Nisole, S., B. Krust, E. Dam, A. Bianco, N. Seddiki, S. Loaec, C. Callebaut, G. Guichard, S. Muller, J. P. Briand, and A. G. Hovanessian.** 2000. The HB-19 pseudopeptide 5[Kpsi(CH2N)PR]-TASP inhibits attachment of T lymphocyte- and macrophage-tropic HIV to permissive cells. AIDS Res. Hum. Retrovir. 16:237–249.
43. **Nisole, S., B. Krust, and A. G. Hovanessian.** 2002. Anchorage of HIV on permissive cells leads to coaggregation of viral particles with surface nucleolin at membrane raft microdomains. Exp. Cell Res. 276:155–173.
44. **Nisole, S., E. A. Said, C. Mische, M. C. Prevost, B. Krust, P. Bouvet, A. Bianco, J. P. Briand, and A. G. Hovanessian.** 2002. The anti-HIV pentameric pseudopeptide HB-19 binds the C-terminal end of nucleolin and prevents anchorage of virus particles in the plasma membrane of target cells. J. Biol. Chem. 277:20877–20886.
45. **Osman, T. A., and K. W. Buck.** 1997. The tobacco mosaic virus RNA polymerase complex contains a plant protein related to the RNA-binding subunit of yeast eIF-3. J. Virol. 71:6075–6082.
46. **Piccininni, S., A. Varaklioti, M. Nardelli, B. Dave, K. D. Raney, and J. E. McCarthy.** 2002. Modulation of the hepatitis C virus RNA-dependent RNA polymerase activity by the non-structural (NS) 3 helicase and the NS4B membrane protein. J. Biol. Chem. 277:45670–45679.
47. **Pietschmann, T., V. Lohmann, G. Rutter, K. Kurpanek, and R. Bartenschlager.** 2001. Characterization of cell lines carrying self-replicating hepatitis C virus RNAs. J. Virol. 75:1252–1264.
48. **Qin, W., H. Luo, T. Nomura, N. Hayashi, T. Yamashita, and S. Murakami.** 2002. Oligomeric interaction of hepatitis C virus NS5B is critical for catalytic activity of RNA-dependent RNA polymerase. J. Biol. Chem. 277:2132–2137.
49. **Qin, W., T. Yamashita, Y. Shirota, Y. Lin, W. Wei, and S. Murakami.** 2001. Mutational analysis of the structure and functions of hepatitis C virus RNA-dependent RNA polymerase. Hepatology 33:728–737.
50. **Quadt, R., C. C. Kao, K. S. Browning, R. P. Hershberger, and P. Ahlquist.** 1993. Characterization of a host protein associated with brome mosaic virus RNA-dependent RNA polymerase. Proc. Natl. Acad. Sci. USA 90:1498–1502.
51. **Randall, G., A. Grakoui, and C. M. Rice.** 2003. Clearance of replicating hepatitis C virus replicon RNAs in cell culture by small interfering RNAs. Proc. Natl. Acad. Sci. USA 100:235–240.
52. **Said, E. A., B. Krust, S. Nisole, J. Svab, J. P. Briand, and A. G. Hovanessian.** 2002. The anti-HIV cytokine midkine binds the cell surface-expressed nucleolin as a low affinity receptor. J. Biol. Chem. 277:37492–37502.
53. **Saito, I., T. Miyamura, A. Ohbayashi, H. Harada, T. Katayama, S. Kikuchi, Y. Watanabe, S. Koi, M. Onji, Y. Ohta, et al.** 1990. Hepatitis C virus infection is associated with the development of hepatocellular carcinoma. Proc. Natl. Acad. Sci. USA 87:6547–6549.
54. **Seeff, L. B.** 1997. Natural history of hepatitis C. Hepatology 26:21S–28S.
55. **Semenkovich, C. F., R. E. Ostlund, Jr., M. O. Olson, and J. W. Yang.** 1990. A protein partially expressed on the surface of HepG2 cells that binds lipoproteins specifically is nucleolin. Biochemistry 29:9708–9713.
56. **Shimakami, T., M. Hijikata, H. Luo, Y. Y. Ma, S. Kaneko, K. Shimotohno, and S. Murakami.** 2004. Effect of interaction between hepatitis C virus NS5A and NS5B on hepatitis C virus RNA replication with the hepatitis C virus replicon. J. Virol. 78:2738–2748.
57. **Shirota, Y., H. Luo, W. Qin, S. Kaneko, T. Yamashita, K. Kobayashi, and S. Murakami.** 2002. Hepatitis C virus (HCV) NS5A binds RNA-dependent RNA polymerase (RdRP) NS5B and modulates RNA-dependent RNA polymerase activity. J. Biol. Chem. 277:11149–11155.
58. **Sinclair, J. F., and A. D. O'Brien.** 2002. Cell surface-localized nucleolin is a eukaryotic receptor for the adhesin intimin-gamma of enterohemorrhagic Escherichia coli O157:H7. J. Biol. Chem. 277:2876–2885.
59. **Srivastava, M., and H. B. Pollard.** 1999. Molecular dissection of nucleolin's role in growth and cell proliferation: new insights. FASEB J. 13:1911–1922.
60. **Take, M., J. Tsutsui, H. Obama, M. Ozawa, T. Nakayama, I. Maruyama, T. Arima, and T. Muramatsu.** 1994. Identification of nucleolin as a binding protein for midkine (MK) and heparin-binding growth associated molecule (HB-GAM). J. Biochem. (Tokyo) 116:1063–1068.
61. **Tsukiyama-Kohara, K., N. Iizuka, M. Kohara, and A. Nomoto.** 1992. Internal ribosome entry site within hepatitis C virus RNA. J. Virol. 66:1476–1483.
62. **Tu, H., L. Gao, S. T. Shi, D. R. Taylor, T. Yang, A. K. Mircheff, Y. Wen, A. E. Gorbalenya, S. B. Hwang, and M. M. Lai.** 1999. Hepatitis C virus RNA polymerase and NS5A complex with a SNARE-like protein. Virology 263: 30–41.
63. **Wakita, T., T. Pietschmann, T. Kato, T. Date, M. Miyamoto, Z. Zhao, K. Murthy, A. Habermann, H. G. Krausslich, M. Mizokami, R. Bartenschlager, and T. J. Liang.** 2005. Production of infectious hepatitis C virus in tissue culture from a cloned viral genome. Nat. Med. 11:791–796.
64. **Wang, C., P. Sarnow, and A. Siddiqui.** 1993. Translation of human hepatitis C virus RNA in cultured cells is mediated by an internal ribosome-binding mechanism. J. Virol. 67:3338–3344.
65. **Wang, Q. M., M. A. Hockman, K. Staschke, R. B. Johnson, K. A. Case, J. Lu, S. Parsons, F. Zhang, R. Rathnachalam, K. Kirkegaard, and J. M. Colacino.** 2002. Oligomerization and cooperative RNA synthesis activity of hepatitis C virus RNA-dependent RNA polymerase. J. Virol. 76:3865–3872.
66. **Weiner, A. J., M. J. Brauer, J. Rosenblatt, K. H. Richman, J. Tung, K. Crawford, F. Bonino, G. Saracco, Q. L. Choo, M. Houghton, et al.** 1991. Variable and hypervariable domains are found in the regions of HCV corresponding to the flavivirus envelope and NS1 proteins and the pestivirus envelope glycoproteins. Virology 180:842–848.
67. **Weiner, A. J., H. M. Geysen, C. Christopherson, J. E. Hall, T. J. Mason, G. Saracco, F. Bonino, K. Crawford, C. D. Marion, K. A. Crawford, et al.** 1992. Evidence for immune selection of hepatitis C virus (HCV) putative envelope glycoprotein variants: potential role in chronic HCV infections. Proc. Natl. Acad. Sci. USA 89:3468–3472.
68. **Yamashita, T., S. Kaneko, Y. Shirota, W. Qin, T. Nomura, K. Kobayashi, and S. Murakami.** 1998. RNA-dependent RNA polymerase activity of the soluble recombinant hepatitis C virus NS5B protein truncated at the C-terminal region. J. Biol. Chem. 273:15479–15486.
69. **Yanagi, M., M. St. Claire, S. U. Emerson, R. H. Purcell, and J. Bukh.** 1999. *In vivo* analysis of the 3′ untranslated region of the hepatitis C virus after *in vitro* mutagenesis of an infectious cDNA clone. Proc. Natl. Acad. Sci. USA 96:2291–2295.
70. **Yang, T. H., W. H. Tsai, Y. M. Lee, H. Y. Lei, M. Y. Lai, D. S. Chen, N. H. Yeh, and S. C. Lee.** 1994. Purification and characterization of nucleolin and its identification as a transcription repressor. Mol. Cell. Biol. 14:6068–6074.
71. **Yi, M., and S. M. Lemon.** 2003. 3′ nontranslated RNA signals required for replication of hepatitis C virus RNA. J. Virol. 77:3557–3568.
72. **Zhong, J., P. Gastaminza, G. Cheng, S. Kapadia, T. Kato, D. R. Burton, S. F. Wieland, S. L. Uprichard, T. Wakita, and F. V. Chisari.** 2005. Robust hepatitis C virus infection *in vitro*. Proc. Natl. Acad. Sci. USA 102:9294–9299.

Cytotoxic T Cell Responses to Human Telomerase Reverse Transcriptase in Patients With Hepatocellular Carcinoma

Eishiro Mizukoshi,[1] Yasunari Nakamoto,[1] Yohei Marukawa,[1] Kuniaki Arai,[1] Tatsuya Yamashita,[1] Hirokazu Tsuji,[1] Kiyotaka Kuzushima,[2] Masafumi Takiguchi,[3] and Shuichi Kaneko[1]

Human telomerase reverse transcriptase, hTERT, has been identified as the catalytic enzyme required for telomere elongation. hTERT is expressed in most tumor cells but seldom expressed in most human adult cells. It has been reported that 80% to 90% of hepatocellular carcinomas (HCCs) express hTERT, making the enzyme a potential target in immunotherapy for HCC. In the current study, we identified hTERT-derived, HLA-A*2402–restricted cytotoxic T cell (CTL) epitopes and analyzed hTERT-specific CTL responses in patients with HCC. Peptides containing the epitopes showed high affinity to bind HLA-A*2402 in a major histocompatibility complex binding assay and were able to induce hTERT-specific CTLs in both hTERT cDNA-immunized HLA-A*2402/K^b transgenic mice and patients with HCC. The CTLs were able to kill hepatoma cell lines depending on hTERT expression levels in an HLA-A*2402–restricted manner and induced irrespective of hepatitis viral infection. The number of single hTERT epitope-specific T cells detected by ELISPOT assay was 10 to 100 specific cells per 3×10^5 PBMCs, and positive T cell responses were observed in 6.9% to 12.5% of HCC patients. hTERT-specific T cell responses were observed even in the patients with early stages of HCC. The frequency of hTERT/tetramer$^+$CD8$^+$ T cells in the tumor tissue of patients with HCC was quite high, and they were functional. In conclusion, these results suggest that hTERT is an attractive target for T-cell–based immunotherapy for HCC, and the identified hTERT epitopes may be valuable both for immunotherapy and for analyzing host immune responses to HCC. (HEPATOLOGY 2006;43:1284-1294.)

Hepatocellular carcinoma (HCC) is the most frequent primary malignancy of the liver and has gained much clinical interest because of its increasing incidence.[1-3] Although current advances in therapeutic modalities have improved the prognosis of HCC patients,[4-6] the survival rate is still not satisfactory. One of the reasons for the poor prognosis is the high rate of recurrence after treatment. To protect against recurrence, tumor antigen-specific immunotherapy is an attractive strategy. Although many tumor-specific antigens have been identified in various cancers, the number of HCC-specific antigens known is still limited.

Human telomerase reverse transcriptase, hTERT, has been identified as the catalytic enzyme required for telomere elongation.[7-10] Recently, several results regarding hTERT-specific cytotoxic T cell (CTL) responses were reported for humans and mice.[11-20] These reports revealed that hTERT-specific CTLs induced by stimulation with peptides or DNA-based immunization kill cancer cell lines that have high levels of hTERT, suggesting that hTERT-reactive T cell clones are not deleted from the human T cell repertoire and that hTERT may be a useful tumor-specific antigen as a target for T-cell–based immunotherapy for cancers. However, the existence of hTERT-specific CTLs and the relationship between immunological

Abbreviations: HCC, hepatocellular carcinoma; hTERT, human telomerase reverse transcriptase; CTL, cytotoxic T cell; HIV, human immunodeficiency virus; PBMC, peripheral blood mononuclear cell; AFP, alpha-fetoprotein; CMV, cytomegalovirus; FCS, fetal calf serum; TIL, tumor infiltrating lymphocyte; PCR, polymerase chain reaction; TRAP, telomerase repeat amplification protocol; IFN-γ, interferon gamma.

From the [1]Department of Gastroenterology, Graduate School of Medicine, Kanazawa University, Kanazawa, Ishikawa, Japan; the [2]Division of Immunology, Aichi Cancer Center Research Institute, Aichi Cancer Center Hospital, Nagoya, Aichi, Japan; and the [3]Division of Viral Immunology, Center for AIDS Research, Kumamoto University, Honjo, Kumamoto, Japan.

Received August 8, 2005; accepted March 20, 2006.

Address reprint requests to: Shuichi Kaneko, M.D., Department of Gastroenterology, Graduate School of Medicine, Kanazawa University, Kanazawa, Ishikawa 920-8641, Japan. E-mail: skaneko@medf.m.kanazawa-u.ac.jp; fax: 81-76-234-4250.

Published online in Wiley InterScience (www.interscience.wiley.com).

DOI 10.1002/hep.21203

Potential conflict of interest: Nothing to report.

responses and clinical factors have not been well characterized in patients with HCC.

In the current study, we first attempted to identify HLA-A*2402–restricted T cell epitopes derived from hTERT and then analyzed hTERT-specific immunological responses in HCC patients.

Patients and Methods

Patient Population. The study examined 72 HLA-A24–positive patients with HCC who were admitted to Kanazawa University Hospital between January 2002 and December 2004, consisting of 48 men and 24 women ranging from 46 to 81 years of age with a mean age of 67 ± 9 years. HCCs were detected by imaging modalities such as dynamic computed tomography (CT) scan, magnetic resonance imaging, and abdominal arteriography. The diagnosis of HCC was histologically confirmed by taking ultrasound-guided needle biopsy specimens in 29 cases, surgical resection in four cases, and autopsy in four cases. For the remaining 35 patients, the diagnosis was based on typical hypervascular tumor staining on angiography in addition to typical findings, which showed hyperattenuated areas in the early phase and hypoattenuation in the late phase on dynamic CT.[21] All subjects were negative for antibodies to human immunodeficiency virus (HIV) and gave written informed consent to participate in this study in accordance with the Helsinki declaration. Eleven healthy blood donors with HLA-A24, who did not have a history of cancer and were negative for hepatitis B surface antigen and anti-HCV antibody, served as controls.

Laboratory and Virologic Testing. Blood samples were tested for hepatitis B surface antigen and HCV antibody by commercial immunoassays (Fuji Rebio, Tokyo, Japan). HLA-based typing of peripheral blood mononuclear cells (PBMCs) from patients and normal donors was performed using complement-dependent microcytotoxicity with HLA typing trays purchased from One Lambda.

The serum alpha-fetoprotein (AFP) level was measured by enzyme immunoassay (AxSYM AFP, Abbott Japan, Tokyo, Japan), and the pathological grading of tumor cell differentiation was assessed according to the general rules for the clinical and pathological study of primary liver cancer.[22] The severity of liver disease (stage of fibrosis) was evaluated according to the criteria of Desmet et al.,[23] using biopsy specimens of liver tissue, where F4 was defined as cirrhosis.

Synthetic Peptides. To identify potential HLA-A24–binding peptides within hTERT, the sequence was reviewed using a computer-based program, which was employed by accessing the World Wide Web site BioInformatics and Molecular Analysis Section for HLA peptide binding predictions (available from http://bimas.cit.nih.gov). The HLA-A24–restricted epitopes derived from HIV envelope protein,[24] cytomegalovirus (CMV) pp65,[25] and HCV NS3 were used as control peptides to test for T cell responses, and the HLA-A2–restricted epitope derived from AFP[26] was used as a control peptide for HLA-A24 stabilization assay as previously described. Peptides were synthesized at Mimotope (Melbourne, Australia) and Sumitomo Pharmaceuticals (Osaka, Japan). They were identified using mass spectrometry, and their purities were determined to be greater than 80% by analytical high-pressure liquid chromatography.

Cell Lines. Three human hepatoma cell lines, HepG2, HuH6, and HuH7, were cultured in Dulbecco's minimum essential medium (Gibco, Grand Island, NY) with 10% fetal calf serum (FCS) (Gibco).

T2-A24 cells, which were T2 cells transfected with HLA-A*2402,[25] were cultured in RPMI 1640 medium containing 10% FCS and 800 μg/mL G418 (GibcoBRL, Grand Island, NY). The HLA-A*2402 gene-transfected C1R cell line (C1R-A24)[27] was cultured in RPMI 1640 medium containing 10% FCS and 500 μg/ml of hygromycin B(Sigma, St Louis, MO), and K562 was cultured in RPMI 1640 medium containing 10% FCS. All media contained 100 U/mL penicillin and 100 μg/mL streptomycin (GibcoBRL, Grand Island, NY).

Plasmid Construction. The plasmid which contains hTERT cDNA was subcloned as previously described.[28] In brief, the EcoRI-SalI fragment containing the hTERT cDNA was subcloned from pCI-Neo-hTERT, which was provided by Dr. Seishi Murakami (Cancer Research Institute, Kanazawa University). The fragment was subcloned into the EcoRI-SalI sites of the plasmid pNKZ-FLAG (pNKZ-FLAG-hTERT).

Injection of hTERT cDNA Into HLA-A*2402/K^b Transgenic Mice. Transgenic mice expressing the α1 and α2 domains from the HLA-A*2402 molecule and the α3 domain from the murine H-2K^b molecule,[29] kindly provided by Sumitomo Pharmaceuticals (Osaka, Japan), were bred in a specific-pathogen–free environment at the animal facility in Kanazawa University. For immunization with the hTERT cDNA, mice were injected with 50 μL cardiotoxin (Latoxan, Rosans, France) (10 μmol/L) per leg into the tibialis anterior muscles on both sides. Five days after injection of the cardiotoxin, the vector pNKZ-FLAG-hTERT containing the hTERT cDNA was injected into the same part of the muscle. Mice immunized with the plasmid pNKZ-FLAG were also used as negative controls. Splenocytes harvested on day 7 after the

Table 1. Characteristics of the Patients Studied

Clinical Diagnosis	No. of Patients	Sex M/F	Age (yr) Mean ± SD	ALT (IU/L) Mean ± SD	AFP (ng/mL) Mean ± SD	Etiology (B/C/Others)	Child-Pugh (A/B/C)	Diff. degree* (Wel/Mod/ Por/ND)	Tumor size** (Large/ Small)	Tumor multiplicity (Multiple/ Solitary)	Vascular Invasion (+/−)	TNM Stage (I/II/IIIA/ IIIB/IIIC/IV)
HCC patients	72	48/24	67 ± 9	66 ± 36	1722 ± 7029	9/59/4	43/25/4	15/21/1/35	44/28	39/33	15/57	30/26/9/1/2/4
Normal donors	11	8/3	35 ± 2	ND	ND	ND	ND	ND	ND	ND	ND	ND

*Histological degree of HCC; wel: well differentiated, mod: moderately differentiated, por: poorly differentiated, ND: not determined.
**Tumor size was divided into either "small" (≤2 cm) or "large" (> 2 cm).

injection of cDNA were tested directly *ex vivo* for IFN-γ production using an ELISPOT assay.

Preparation of PBMCs and Tumor-Infiltrating Lymphocytes. PBMCs were isolated as previously described.[30,31] Fresh PBMCs were used for the CTL assay, and the remaining PBMCs were resuspended in RPMI 1640 medium containing 80% FCS and 10% dimethyl sulfoxide (Sigma, St. Louis, MO) and cryopreserved until used. Tumor-infiltrating lymphocytes (TILs) were isolated by mechanical homogenization of tumors, which were resected by surgical treatment and cryopreserved as described until used.

Major Histocompatibility Complex Binding Assay. Peptide binding assays were performed as previously described.[31,32] The data were expressed as % mean fluorescence intensity (MFI) increase, which was calculated as follows: Percent MFI increase = (MFI with the given peptide − MFI without peptide)/(MFI without peptide) × 100.

ELISPOT Assay. ELISPOT assays were performed as previously described[31] with the following modifications. Three hundred thousand unfractionated PBMCs or 100,000 TILs with 10,000 T2-A24 cells were added in duplicate cultures of RPMI 1640 medium containing 5% FCS together with the peptides at 10 μg/mL. For the mouse assay, 2×10^5 spleen cells were used for each well. The number of specific spots was determined by subtracting the number of spots in the absence of antigen from that in the presence of antigen. Responses were considered positive for the human ELISPOT assay if more than 10 specific spots were detected and if the number of spots in the presence of antigen was at least twofold greater than that in the absence of antigen.

Cytotoxicity Assay. hTERT-derived peptide-specific T cells were expanded from PBMCs in 96-well round-bottomed plates (NUNC, Naperville, IL) as previously described.[30] Briefly, 400,000 cells per well were stimulated with 10 μg/mL synthetic peptide, 10 ng/mL rIL-7, and 100 pg/mL rIL-12 (Sigma) in RPMI 1640 medium supplemented with 10% heat-inactivated human AB serum, 100 U/mL penicillin, and 100 μg/mL streptomycin. The cultures were re-stimulated with 10 μg/mL peptide, 20 U/mL of rIL-2 (Sigma) and 1×10^5 mytomicin C-treated autologous PBMCs on days 7 and 14. On days 3, 10, and 17, 100 μL RPMI with 10% human AB serum and 10 U/mL rIL-2 (final concentration) were added to each well. Cytotoxicity assays were performed as previously described.[31]

Tetramer Staining and Flow Cytometry. Peptide $hTERT_{461}$-specific tetramer was purchased from Medical Biological Laboratories Co., Ltd (Nagoya, Japan). Tetramer staining was performed as previously described.[33] In brief, PBMCs and TILs were stained with CD4-FITC, CD14-FITC, CD19-FITC, CD8-PerCP (BD PharMingen, San Diego, CA), and tetramer-PE (10 μL) for 30 minutes at room temperature. Cells were washed, fixed with 0.5% paraformaldehyde/phosphate-buffered saline, and analyzed on a FACSCalibur flow cytometer. Data analysis was undertaken with CELLQuest software (Becton Dickinson, San Jose, CA).

Telomerase Assay. Telomerase activity was measured by two methods according to the manufacturer's directions. First, a polymerase chain reaction (PCR)-based telomerase repeat amplification protocol (TRAP) assay was carried out with a TRAPEZE ELISA telomerase detection kit (Intergen Co. Ltd., Auckland, New Zealand). The products of the PCR were fractionated by electrophoresis on a 10% polyacrylamide gel and then visualized by staining with SYBR-Green I (Molecular Probes, Eugene OR). Second, a TRAP enzyme-linked immunosorbent assay (ELISA) was used to quantitatively measure telomerase activity with a TRAPEZE ELISA telomerase detection kit (Intergen Co. Ltd.). Cell extracts were prepared from HepG2, HuH6, and HuH7 cells and used at 0.01 μg per assay. Telomerase activity was also measured in the tumor of 10 patients with HCC who received surgical treatment. Cell extracts were prepared from resected tumors and used at 0.1 μg per assay.

Statistical Analysis. Fisher's exact test (2-sided *P*-value) and the unpaired Student's *t* test were used to analyze the effect of variables on immune responses in HCC patients.

Results

Patient Profiles. The clinical profiles of the patients are shown in Table 1. The tumors of 37 patients were